Deep mutational scanning reveals tail anchor characteristics important for mitochondrial targeting

Abdurrahman Keskin[*†], Emel Akdoğan[*], Cory D. Dunn[*‡]

[*] Department of Molecular Biology and Genetics, Koç University, Sarıyer, İstanbul, Turkey

[†] Current affiliation:
Department of Biological Sciences
Columbia University
New York, NY 10027

[‡] Corresponding author
Dr. Cory Dunn
Koç Üniversitesi
Fen Fakultesi
Rumelifeneri Yolu
Sarıyer, İstanbul 34450
Turkey
Email: cdunn@ku.edu.tr
Phone: +90 212 338 1449
Fax: +90 212 338 1559

Running head: Comprehensive analysis of Fis1 TA

Abbreviations: TA, tail anchor; OM, outer membrane; MAD, membrane-anchoring domain; 3-AT, 3-aminotriazole; CHX, cycloheximide

ABSTRACT:

Proteins localized to mitochondria by a carboxyl-terminal tail anchor (TA) play roles in apoptosis, mitochondrial dynamics, and mitochondrial protein import. To reveal characteristics of TAs that are important for mitochondrial targeting, we examined the TA of the *Saccharomyces cerevisiae* Fis1 protein. We generated a library of Fis1p TA variants fused to the Gal4 transcription factor, then selected for mutations allowing Gal4 activity in the nucleus. Next-generation sequencing allowed quantification of TA variants in our mutant library both before and after selection for reduced TA targeting. High-throughput results were confirmed by further analysis of individual Fis1p TA mutants. Intriguingly, positively charged residues were more acceptable at several positions within the membrane-associated domain of the Fis1p TA than negatively charged residues. These findings provide strong, *in vivo* evidence that lysine and arginine can "snorkel," stably associating with a lipid bilayer by placing their terminal charges at the membrane interface. Our work provides the first high-resolution analysis of an organelle targeting sequence by deep mutational scanning.

INTRODUCTION:

Proteins inserted within the mitochondrial outer membrane (OM) by a carboxyl-terminal tail anchor (TA) are important for programmed cell death, mitochondrial protein import, and the control of mitochondrial shape and number (Wattenberg and Lithgow, 2001). However, how proteins are targeted to mitochondria by TAs is not understood (Lee *et al.*, 2014; Neupert, 2015). TA targeting seems to depend upon incompletely defined structural characteristics of the TA rather than a defined consensus sequence (Beilharz, 2003; Rapaport, 2003; Borgese *et al.*, 2007). No components dedicated to TA insertion have been identified, and in fact, genetic and biochemical evidence suggest that spontaneous insertion of TAs might occur without the need for a translocation machinery (Setoguchi *et al.*, 2006; Kemper *et al.*, 2008). Such a mode of insertion stands in stark contrast with TA protein insertion into the endoplasmic reticulum (ER), which can take advantage of a conserved set of soluble proteins and membrane-bound receptors (Denic *et al.*, 2013; Johnson *et al.*, 2013).

Genetic selection schemes using the organism *Saccharomyces cerevisiae* have been of high value in understanding how proteins reach their proper destination within the eukaryotic cell. During such studies, a protein required for survival under selective conditions can be mislocalized, and thereby made inactive, by a targeting sequence utilized by the transport process being studied. Next, mutations that allow return of this mistargeted protein to a region of the cell at which it can perform its function are recovered under selective conditions. *Trans* factors related to protein targeting are identified by standard genetic approaches. Alternatively, *cis* mutations in the targeting sequence are revealed, typically by Sanger sequencing of individual fusion construct clones. Most prominently, this genetic approach to studying protein targeting and transport has been important in understanding protein transit to and through the endomembrane system (Deshaies and Schekman, 1987; Robinson *et al.*, 1988; Stirling *et al.*, 1992). This approach has also been applied to the study of protein import and

74 export at the mitochondrial inner membrane (Jensen *et al.*, 1992; Maarse *et al.*, 1992;
75 He and Fox, 1999).
76
77 Even with the availability of powerful genetic strategies, a fine-grained analysis of any
78 single eukaryotic protein targeting signal has been lacking. However, with the advent of
79 next-generation sequencing, more comprehensive studies of protein targeting
80 sequences are possible. In this study, we successfully coupled genetic selection to
81 next-generation sequence analysis in order to reveal the structural and sequence
82 characteristics important for localization of the tail-anchored Fis1 protein to the
83 mitochondrial OM.
84

RESULTS:

Localization to the mitochondrial outer membrane via the Fis1 tail anchor prevents Gal4-mediated transcriptional activation

The TA of Fis1p is necessary (Mozdy *et al.*, 2000; Beilharz, 2003) and sufficient (Kemper *et al.*, 2008; Förtsch *et al.*, 2011) for insertion of this polypeptide into the mitochondrial OM. Fis1p has been suggested to reach a final topology in the outer membrane in which the amino-terminal bulk of the protein faces the cytosol, a very short and positively charged carboxyl-terminus protrudes into the mitochondrial intermembrane space, and the two are connected by a membrane-anchoring domain (MAD) passing through the OM (Mozdy *et al.*, 2000). In developing our selection for TA mutations that diminish Fis1p targeting, we reasoned that fusion of a transcription factor to Fis1p would lead to insertion within the mitochondrial OM and a lack of nuclear function (Figure 1A). Mutations within the TA of Fis1p that prevent effective membrane insertion would, however, presumably allow the linked transcription factor to enter the nucleus, promote expression of its targets, and allow survival under specific selective conditions. Toward this goal, we fused the Gal4 transcription factor to the amino-terminus of full-length Fis1p, since *S. cerevisiae* strains allowing titratable selection based upon Gal4p potency are readily available. We included superfolder GFP (Pédelacq *et al.*, 2005) between the Gal4 and Fis1 moieties, and upon overexpression, GFP fluorescence was visible at mitochondria (Figure S1). Importantly, the Gal4-Fis1p fusion failed to complement the mitochondrial morphology defect of a *fis1Δ* mutant (Figure S1 and unpublished results), suggesting that our fusion protein cannot interact effectively with other mitochondrial division components that might potentially impede nuclear translocation of Gal4-Fis1p upon TA mutation.

To assess failed Gal4-Fis1p targeting to mitochondria, we specifically took advantage of the Gal4-driven *HIS3* and *URA3* auxotrophic markers in MaV203, a strain commonly used for yeast-two-hybrid assays (Vidal *et al.*, 1996a). Similar to cells containing an

empty vector, Gal4p fused to Fis1p was unable to provide growth on medium lacking histidine and containing 20mM 3-aminotriazole (3-AT) to competitively inhibit any His3p produced independently of Gal4p activation (Durfee *et al.*, 1993) or in medium lacking uracil (SC-Ura) (Figure 1B). However, the same Gal4-Fis1 polypeptide devoid of its TA [Gal4-Fis1(ΔTA)] provided ample proliferation on the same two selective media. This result indicated that our fusion protein could translocate to the nucleus upon TA disruption and that any potential lipid binding mediated by the cytosolic domain of Fis1p (Wells and Hill, 2011) will not prevent genetic assessment of TA localization.

Following validation of our experimental approach, we immediately sought mutations in the TA that would block targeting of Gal4-Fis1p to the mitochondrial OM by isolating colonies spontaneously arising on medium lacking uracil. Limited sequencing of the constructs encoding Gal4-Fis1p within these isolates revealed at least seven nonsense and 19 frameshift mutations out of a total of 32 plasmids analyzed. While these findings further validated the link between growth under selective conditions and damage to the Fis1p TA, continued encounters with nonsense and frameshift mutations would not be greatly informative regarding the sequential or structural determinants important for TA targeting.

In the strain used for our selective scheme, a Ura^+ phenotype requires greater Gal4-dependent transcriptional activation than a His^+ phenotype (Vidal *et al.*, 1996b). Therefore, we reasoned that initial selection of TA mutants based on a His^+ phenotype may provide informative mutations that weaken, but do not totally inhibit membrane association. We used mutagenic PCR to generate altered TAs within the context of a Gal4-Fis1 fusion protein. We then isolated four colonies that proliferated upon SMM-His medium containing 20mM 3-AT, yet exhibited diminished proliferation on SC-Ura medium when compared to cells expressing the Gal4-Fis1(ΔTA) polypeptide. Sanger sequencing of the region encoding the TA of Gal4-Fis1p within these colonies revealed one clone with a V145E mutation (amino acid numbering provided in this study will correspond to that of the unmodified, full-length Fis1 protein), two clones with a L139P

mutation, and one clone with two mutations: L129P and V138A. Serial dilution assays (Figure 2A) confirmed that V145E and L139P provided a less than maximal, but still apparent Ura$^+$ phenotype, with the V145E mutant allowing more rapid proliferation on medium lacking uracil than the L139P mutant. The L129P/V138A mutant provided a His+ phenotype, but could not drive uracil prototrophy, suggesting a less severe localization defect than that exhibited by the other two mutant TAs. Interestingly, the V145E mutation falls within the MAD of the Fis1p TA, consistent with poor accommodation of a charged amino acid within this hydrophobic stretch of amino acids. Moreover, the Fis1p TA is predicted to be mostly alpha-helical in nature, so isolation of the potentially helix-disrupting L139P replacement by selection may indicate a need for TA helicity during mitochondrial targeting.

We then verified that these mutations presumably disrupting TA targeting are not isolated merely as a consequence of the Gal4p-based selection system that we had applied. Toward this goal, we took advantage of the Pdr1 transcription factor, which promotes resistance to several drugs (Meyers *et al.*, 1992; Prasad and Goffeau, 2012). The *PDR1-249* allele encodes a hyperactive Pdr1p that promotes cycloheximide (CHX) resistance (Mutlu *et al.*, 2014). Fusion of the hyperactive Pdr1-249 protein to the unmutated Fis1p TA did not allow CHX resistance (Figure S2). However, addition of the V145E mutation to the TA in this fusion protein did permit CHX resistance, presumably as Pdr1-249p entered the nucleus to activate its targets. These findings demonstrate that mutations recovered using our Gal4p-based scheme are unlikely to be related to the use of any specific transcription factor.

Transcription driven by Gal4-Fis1p indirectly reports on TA targeting to mitochondria and may be affected by mutant stability, ability of the fusion protein to translocate to the nucleus, or other events unrelated to normal TA localization. To further examine whether isolated TA mutations affect mitochondrial OM targeting, we linked wild-type (WT) or mutant Fis1p TAs to the carboxyl-terminus of mCherry. To assess mitochondrial localization of these fusion proteins, mitochondria were specifically

labelled with GFP targeted to mitochondria by the presequence of the Cox4 protein (Sesaki and Jensen, 1999). Importantly, the TA of Fis1p lacks information required for mediating mitochondrial fragmentation (Habib *et al.*, 2003), indicating that the localization of these constructs should not be influenced by interaction partners of full-length, inserted Fis1p.

The location of mCherry fused to Fis1p TAs faithfully recapitulated our genetic findings. V145E and L139P mutations in the Fis1p TA led to very substantial cytosolic localization of mCherry (Figure 2B). Moreover, the L129P/V138A TA, consistent with its weaker activation of Gal4 targets in our selection system, provided still discernable mitochondrial localization of the mCherry signal, but cytosolic levels of this mutant fusion protein appeared to be increased compared to mCherry fused to the WT TA. These results suggest that, in general, our genetic approach is likely to accurately report upon the ability of the Fis1p TA to moor proteins to the mitochondrial outer membrane.

Deep mutational scanning uncovers determinants of Fis1p tail-anchor targeting

Buoyed by our initial isolation of TA mutations affecting mitochondrial localization, we decided to take a more global approach to the analysis of the Fis1p TA. Using degenerate primers and recombination-based cloning in *S. cerevisiae*, we sought to generate a library consisting of all possible codons at every one of 27 amino acid positions within the TA of Gal4-Fis1p. We then allowed the pool of cells containing mutant TAs to divide four times under six possible culture conditions: no specific selection for *HIS3* or *URA3* reporter activation (SC-Trp, selecting only for plasmid maintenance), selection for *HIS3* activation at different 3-AT concentrations (SMM-Trp-His +0, 5, 10, or 20mM 3-AT), or selection for *URA3* activation (SC-Ura). Plasmid DNA was isolated from each pool of mutants, and TA coding sequences were amplified and subjected to next-generation sequencing. We then focused our analysis only on those clones within our pools that carried zero or one amino acid changes.

While all potential replacement mutations could not be detected within our starting library (Figure S3), and some biases did exist at each TA position, most potential amino acid mutations were represented within our pool. 98.9% of potential amino acid replacements were identified in the starting pool cultured in SC-Trp, and 95.9% of TAs with single mutations were represented by at least 10 counts. Quantification of counts from all samples can be found in Table S1. When comparing the mutant pool cultured in SC-Trp with selection in SMM-Trp-His without added 3-AT, there was no appreciable difference in the relative abundance of most mutant TAs, including truncation mutations expected to totally prevent mitochondrial targeting of Gal4-Fis1p (Figure S4A). Such a result is consistent with 'leaky' expression of *HIS3* independent of Gal4-driven activation (Durfee *et al.*, 1993). However, upon addition of 3-AT at concentrations of 5mM (Figure S4B), 10mM (Figure S4C), or 20mM (Figure 3) to medium lacking histidine, there were substantial shifts in the composition of the mutant pools toward specific amino acids, prompting further experiments that we describe below. The pool cultured in SC-Ura medium showed very strong selection for nonsense mutations within the TA (Figure S4D), but less prominent biases among amino acids. When considering our initial findings, in which recovery of uracil prototrophs by our genetic scheme led to a high recovery of frameshift and nonsense mutations, assessment of *HIS3* activation seems more informative regarding determinants of Fis1p TA targeting than competition assays performed in the more strongly selective medium lacking uracil.

Independently of the primary amino acid sequence, the specific codons used to direct synthesis of a protein can affect that polypeptide's translation rate and folding (Yu *et al.*, 2015). Although TAs shorter than the ribosome exit tunnel, which is 30 to 40 residues in length (Voss *et al.*, 2006), must certainly be inserted post-translationally, we also examined enrichment of specific codons following selection for Gal4-Fis1p presence in the nucleus. However, this approach did not provide notable evidence of a role for specific codons in directing localization of the Fis1p TA (Figure S5). While the data are more 'noisy' due to a lack of representation of certain codons at each

position, codons encoding the same amino acid generally acted in concert with one another within our selection scheme, placing our focus on the amino acid sequence of library variants rather than on codon sequence.

Proline is not acceptable at many locations within the Fis1p tail anchor

Previous analyses of tail-anchored mitochondrial proteins suggested that primary sequence may not determine TA insertion (Beilharz, 2003; Rapaport, 2003; Borgese *et al.*, 2007). Importantly, our global analysis demonstrates no apparent requirement for a single, specific amino acid at any given position within the TA in order to achieve membrane localization; most amino acid replacements within the WT TA sequence fail to lead to selectable reporter activation (Figure 3). We focused our subsequent analysis on general characteristics of the TA that might be important for mitochondrial OM targeting.

The recovery of the L139P mutation during preliminary selection for Fis1p TA mutations indicated that proline may not be acceptable within the hydrophobic core of the Fis1p TA. Our deep mutational scan of the Fis1p TA in SMM-Trp-His+20mM 3-AT (Figure 3) also strongly indicated that proline insertion across many positions disrupted mitochondrial TA localization. When focusing specifically upon those mutants that were in the top 75% most commonly counted variants in the starting pool (>126 counts) and enriched at least four-fold in SMM-Trp-His + 20mM 3-AT, 12 of 33 missense mutations within this set were proline replacements (Figure 4), further indicating failure of TA targeting following placement of proline at many TA positions.

Subsequently, we carried out directed experiments to further examine poor accommodation of proline within the Fis1p TA. We further studied the L139P mutant that was initially isolated during selection for Fis1p TA targeting mutants, and we also generated four additional, individual proline replacements within Gal4-Fis1p and tested for Gal4-driven reporter activation. Newly constructed V134P, L139P, A140P, and

A144P substitutions, consistent with our larger scale analysis (Figure 3 or Figure 4), provided ample proliferation on medium selective for *HIS3* activation (Figure 5A). We noted that only the A144P substitution mutation provided strong proliferation on medium lacking uracil (Figure S6A). Upon visualization of mCherry fused to these Fis1p TA mutants, V134P, L139P, A140P, and A144P replacements all clearly diminished mCherry localization to mitochondria (Figure 5B). Our results suggest that the secondary structure of the Fis1p TA is important for its function, and that disruption of helicity at many locations may make targeting to the mitochondrial OM unfavorable.

Curiously, the G137P mutation was not strongly enriched within the mutant pool during selection (Figure 3). Consistent with these results, individual testing of this mutant suggested poor activation of Gal4-dependent transcription (Figure 5A). Moreover, mCherry fused to a Fis1p TA containing the G137P mutation remained strongly localized to mitochondria (Figure 5B). Therefore, proline seems permissible at specific positions within the MAD of the Fis1p TA.

For those mutant Fis1p TAs that cannot effectively direct mCherry to mitochondria, two mechanisms may explain failure of mitochondrial localization. First, targeting to and insertion at mitochondria may be impeded. Second, these mutant TAs may support initial mitochondrial translocation, but a lack of stability within the lipid bilayer may lead to ejection from the mitochondrial OM by a quality control mechanism. Recently, the yeast Msp1 protein and its human ortholog ATAD1, have been identified as potential 'extractases' that can remove improperly folded or mislocalized proteins from the mitochondrial OM (Chen *et al.*, 2014; Okreglak and Walter, 2014). We tested whether any of tail-anchored fluorescent proteins containing proline replacements and not strongly localized to mitochondria could recover mitochondrial localization in cells deleted of Msp1p. However, deletion of Msp1p did not lead to relocalization of any tested mutant mCherry-TA fusion protein to mitochondria (Figure 5C), providing no evidence for proper targeting, then subsequent removal, of assayed Fis1p TAs harboring proline replacements.

295 *Extension or reduction of Fis1p TA length does not affect targeting to mitochondria*
296
297 Targeting of tail-anchored proteins to specific membranes has been suggested to
298 depend, at least in part, upon the specific length of the MAD domain within the TA
299 (Isenmann *et al.*, 1998; Horie *et al.*, 2002). We reasoned that the region within the MAD
300 at which prolines do not strongly disrupt mitochondrial targeting may be amenable to
301 the insertion or deletion of new amino acids, thereby allowing us to test the relationship
302 between Fis1p TA length and mitochondrial targeting. We inserted one (∇1A), two
303 (∇2A), or three (∇3A) additional alanines between A135 and G136 within the TA of Gal4-
304 Fis1p, but none of these mutant constructs led to apparent *HIS3* (Figure 6A) or *URA3*
305 (Figure S6B) activation. We then analyzed the location of mCherry fused to a Fis1p TA
306 carrying these same insertions. All constructs were localized properly to mitochondria
307 (Figure 6B).
308
309 Next, we deleted one (ΔG136), two (ΔA135-G136), or three (ΔA135-G137) amino acids
310 within the Fis1p MAD and performed similar assays. Like our insertion mutants,
311 deletion mutants were apparently targeted to a membrane, as assessed by Gal4-driven
312 reporter transcription (Figure 6A and Figure S6B). Moreover, mCherry remained
313 localized to mitochondria when up to three amino acids were deleted (Figure 6C).
314
315 Disruption of the ER-localized Spf1 protein reduces the contrast in ergosterol content
316 between the ER and the mitochondrial OM (Krumpe *et al.*, 2012). Consequently, TAs
317 normally localized to mitochondria are mistargeted to the ER upon Spf1p deletion. The
318 sterol concentration of membranes can determine bilayer thickness (Dufourc, 2008),
319 raising the possibility that insertions or deletions may allow mitochondrial TAs to once
320 again prefer mitochondrial OM targeting over ER localization in the *spf1Δ* background.
321 However, mCherry linked to insertion or deletion mutants of the Fis1p TA remained
322 prominently localized to the ER in mutants lacking Spf1p (Figure S7).
323

Together, our results demonstrate that the Fis1p TA is targeted to mitochondria even when its length is substantially altered.

The hydrophilic carboxyl-terminus of the tail anchor allows specific targeting to mitochondria

Analysis of the data from our deep mutational scan suggested that nonsense mutations throughout much of the TA can allow Gal4-Fis1p to move to the nucleus and activate transcription (Figure 3, Figure 4, and Figure S4). Stop codons placed within the highly charged RNKRR pentapeptide near the carboxyl-terminus of Fis1p, however, seem to permit some membrane localization as reported by proliferation in selective medium. Therefore, we examined the behavior of a R151X mutant, which lacks all charged amino acids following the predicted MAD. Supporting partial localization to a cellular membrane, the R151X mutant of Gal4-Fis1p did not activate Gal4-controlled expression of *HIS3* to the same extent of a Gal4-Fis1p construct lacking the entire TA (Figure 7A), nor did the R151X mutation lead to proliferation on medium lacking uracil (Figure S6C). Consistent with those results, the R151X TA directed mCherry to intracellular organelles (Figure 7B). However, along with some apparent mitochondrial association, the R151X TA was also clearly localized to the ER. Interestingly, ER localization of mCherry fused to the R151X TA occurred independently of Get3p, a receptor for ER tail-anchored proteins (Schuldiner *et al.*, 2008), suggesting an alternative, parallel pathway for localization of the R151X TA to the ER (Figure S8). Our results demonstrate that the charged amino acids at the carboxyl-terminus of the TA provide organelle specificity, yet are not totally required for membrane localization. These findings are consistent with previous results reporting that positively charged amino acids following the MAD of Fis1p allow mitochondrial targeting of TAs (Isenmann *et al.*, 1998; Kuroda *et al.*, 1998; Borgese *et al.*, 2001; Stojanovski *et al.*, 2004), perhaps by decreasing total TA hydrophobicity, a factor important for determining the final location of a TA (Beilharz, 2003; Wattenberg *et al.*, 2007).

Since the R151X variant of Gal4-Fis1p activated Gal4-driven reporters, yet was at least partially localized to the ER, we wondered if ER localization of any protein fused to Gal4 might similarly lead to Gal4-driven transcription due to the physical continuity between the ER and nuclear envelope. Therefore, we examined the TA of the human FIS1 protein (hFIS1), since full-length hFIS1 can localize to ER in *S. cerevisiae* (Stojanovski *et al.*, 2004). Indeed, we found that mCherry fused to the hFIS1 TA was mostly localized to ER (Figure S9A). However, a fusion protein consisting of Gal4 fused to the TA of hFIS1 did not provide *HIS3* activation (Figure S9B), indicating that the hFIS1 TA is quantitatively membrane-targeted in *S. cerevisiae* and that activation of Gal4-dependent reporters upon removal of the positively charged carboxyl-terminus from Gal4-Fis1p is unlikely to be a consequence of ER localization.

Due to the mislocalization of the hFIS1 TA, we then investigated the possibility that other mitochondrial TA proteins from human would be targeted improperly in *S. cerevisiae*. We fused mCherry to the TA of human BAX, a region that is sufficient for insertion at the mammalian mitochondrial OM (Schinzel *et al.*, 2004). While mCherry signal was diminished in comparison with other mCherry fusion proteins examined in this study and expressed under the same promoter, mCherry fused to the BAX TA was properly targeted to mitochondria (Figure S9C). Gal4 fused to the BAX TA did not activate selectable reporters (C. Dunn, unpublished results), suggesting effective mitochondrial targeting mediated by the BAX TA.

Positively charged amino acids are more acceptable than negatively charged amino acids within the predicted transmembrane domain of the Fis1p tail anchor

Our deep mutational scan of the Fis1p TA demonstrated that Gal4-Fis1p was generally able to activate gene expression when aspartate or glutamate was placed within the MAD (Figure 3). In fact, upon examination of those amino acid replacements found within the top three quartiles of counts in the initial library and also enriched at least four-fold upon culture in SMM-Trp-His + 20mM 3-AT, 18 of 33 missense mutations

were aspartate or glutamate substitutions (Figure 4). We were surprised to find that placement of positively charged arginine or lysine residues appeared to be much more acceptable within the MAD of Fis1p than aspartate or glutamate; none of the amino acid substitutions within the high-count, high-enrichment set (Figure 4) derived under selective conditions were by lysine or arginine.

To further pursue the possibility that positively charged amino acids can be accommodated within the Fis1p MAD, we mutated four amino acids within the hydrophobic stretch of the Fis1p TA to aspartate, glutamate, lysine, or arginine. Specifically, we generated amino acid replacements at positions V132, A140, A144, or F148, then retested these mutants under selection for Gal4-Fis1p transcriptional activity. The results from our global analysis were verified, with aspartate and glutamate mutations providing stronger reporter activation than lysine and arginine mutations (Figure 8). Only the A144D mutation provided sufficient Gal4 activation for proliferation on medium lacking uracil (Figure S6D), suggesting a very severe TA localization defect caused by this TA mutation. We noted that these mutant Gal4-Fis1 constructs exhibit altered behavior at different temperatures. For example, lysine substitutions clearly led to comparably elevated *HIS3* activity at 18˚C at positions A140 and F148 (Figure S10A), and glutamate substitutions may provide moderately reduced *HIS3* activity when compared to aspartate substitutions upon incubation at 37˚C (Figure S10B). This outcome is consistent with the idea that altered phospholipid dynamics at different temperatures may lead to consequent changes to TA insertion efficiency (de Mendoza and Cronan, 1983).

We then tested the ability of these charged Fis1p TAs to promote mitochondrial localization of mCherry. At V132 and F148, positions within the MAD nearer to the putative water-lipid bilayer interface, mutation to positively charged amino acids allowed abundant localization to mitochondria (Figure 9A). In contrast, mutation to negatively charged amino acids clearly hindered mitochondrial targeting. We noted that F148D and F148E replacements hampered mitochondrial localization more severely

than V132D and V132E replacements. At position A144, lying more deeply within the MAD, all charge mutations inhibited mCherry targeting to mitochondria to some degree, but TAs containing A144D and A144E were less able to localize to mitochondria than A144K or A144R. Finally, no mitochondrial localization was apparent for any of the charge mutants tested at position A140. However, A140K and A140R mutants differed from A140D and A140E mCherry-TA mutants by localizing to other membranes within the cell, including the plasma membrane, rather than providing a diffuse cytosolic signal. Taken together, our results demonstrate that positively charged amino acids at several mitochondrial TA positions do not prohibit mitochondrial targeting and are clearly more acceptable than negatively charged amino acids at those same positions.

We then tested whether deletion of the OM extractase Msp1p might allow those charged Fis1p TAs that poorly localize to mitochondria to recover their targeting to this organelle. However, Msp1p removal did not permit relocalization of tail-anchored fluorescent proteins to mitochondria (Figure 9B), supporting the idea that charge replacements within the Fis1p TA lead to a failure of association with the OM rather than enhanced removal from mitochondria.

We carried out assays to determine if Fis1p carrying charge mutations within their TAs at V132, A144, or V148 can provide Fis1p activity. Negligible Fis1p activity at mitochondria is apparently sufficient to promote mitochondrial fission (Habib *et al.*, 2003; Krumpe *et al.*, 2012), suggesting that even minimal localization and related functionality at the OM would be detectable by functional assays. For example, when Fis1p activity is absent, mitochondrial fission cannot proceed and unchecked fusion leads to a unified mitochondrial network (Mozdy *et al.*, 2000). Interestingly, Fis1p variants harboring charged residues, positive or negative, at positions V132, A144, or V148 provided some Fis1p function when expressed from a plasmid in a *fis1Δ* background, with the exception of the Fis1p carrying the A144D mutation, as indicated by mitochondrial morphology (Figure 10A). To further investigate Fis1p activity,

mitochondrial morphology was further perturbed by treatment with sodium azide, which leads to mitochondrial fragmentation in cells competent for mitochondrial division (Fekkes *et al.*, 2000; Klecker *et al.*, 2015) and to facile visualization of mitochondrial fission defects. Again, except for the A144D mutant, all Fis1p variants tested were able to provide mitochondrial division activity (Figure 10B and Figure S11).

Next, we applied a genetic test of Fis1p function. When mitochondrial fusion is blocked, unbalanced mitochondrial division leads to mitochondrial fragmentation (Hermann *et al.*, 1998; Rapaport *et al.*, 1998) and consequent loss of mtDNA and the ability to respire. If mitochondrial division is lacking, however, mtDNA is instead maintained by cells unable to carry out mitochondrial fusion (Sesaki and Jensen, 1999; Fekkes *et al.*, 2000; Mozdy *et al.*, 2000; Tieu and Nunnari, 2000). In a result consistent with our microscopy-based analysis, we found that only the A144D variant of Fis1p lacked activity and therefore allowed cells to maintain mtDNA when the mitochondrial fusogen Fzo1p is removed (Figure 10C). All other variants provided sufficient fission activity for mitochondrial fragmentation and consequent mtDNA loss in the absence of Fzo1p. We note that upon selection for Gal4-driven reporter activation, only the A144D charge mutant provided sufficient *URA3* activation for proliferation on medium lacking uracil (Figure S6D), supporting the correspondence between each mutant TA's targeting, as reported by Gal4-Fis1p transcriptional activity, and its functionality at the mitochondrial surface. Taken together, our results demonstrate that positively charged amino acids within the MAD can better promote Fis1p localization than negatively charged amino acids, but that even negatively charged amino acids can be accommodated within the MAD and lead to some low level of mitochondrial targeting.

DISCUSSION:

Using a deep mutational scanning approach, we explored structural characteristics of the Fis1p TA important for targeting to the mitochondrial outer membrane. To our knowledge, this work is the first application of this technique to the study of a eukaryotic organelle targeting signal. Deep mutational scanning, when coupled to an effective method of screening or selection, is very cost- and time-effective (Araya and Fowler, 2011; Boucher *et al.*, 2014; Fowler and Fields, 2014). Mutant library generation, subsequent pool selection, and next-generation sequencing were completed in just a few months. Consequently, this approach generates far more useful data over a shorter duration than, for example, alanine scanning mutagenesis or low-throughput genetic selection followed by Sanger sequencing. Deep mutational scanning has recently been applied successfully to other areas of study, such as membrane protein insertion within bacteria (Elazar *et al.*, 2016), tumor suppressor structure and function (Starita *et al.*, 2015), and the relationship between a polypeptide's evolutionary path and its present fitness (Hietpas *et al.*, 2011; Melamed *et al.*, 2013).

Positively charged amino acids within membrane inserted protein segments may "snorkel" to the lipid bilayer surface

Because there is a high energetic barrier to placing any charged residue into a lipid bilayer (Cymer *et al.*, 2015), we were initially surprised to find that positively charged amino acids within the MAD of the Fis1p TA promoted mitochondrial targeting far better than negatively charged amino acids. However, it has been suggested that lysine and arginine within a MAD can "snorkel," or integrate the uncharged portion of their side chain into the hydrophobic milieu of the lipid bilayer and locate their positive charges near polar head groups at the interface between the membrane and aqueous environment (Segrest *et al.*, 1990; Monné *et al.*, 1998; Strandberg and Killian, 2003; Schow *et al.*, 2010). Some phospholipid head groups carry a net negative charge, potentially providing further favorability to snorkeling lysine and arginine. The shorter

hydrophobic portion of aspartate and glutamate, however, may not permit the side chain to easily reach the membrane interface in order to remove the negative charge from the hydrophobic environment, and if they do reach the lipid bilayer surface, charge repulsion might make such a conformation unfavorable. Snorkeling has been visualized, for instance, during structural studies of the Kv1.2 potassium channel (Long *et al.*, 2005) and integrin β3 (Kim *et al.*, 2012). However, little *in vivo* or functional evidence has been reported supporting the snorkeling of amino acids located within MADs. Our deep mutational scan of the Fis1p TA, a region dedicated only to the process of mitochondrial OM integration (Habib *et al.*, 2003; Kemper *et al.*, 2008), strongly suggests the ability of lysine or arginine to be accommodated by snorkeling at numerous positions within the Fis1p MAD. We note that snorkeling, if operative for positive charges within the Fis1p TA, may not be permitted within the context of all mitochondrial TAs: replacement of S184 within the BAX TA by lysine does not seem to permit mitochondrial localization of this protein (Nechushtan *et al.*, 1999).

Further deep mutational scans of MADs may further support the concept of snorkeling. Interestingly, since those Fis1p TAs mutated to contain positively charged amino acids within the MAD were not targeted to the OM with full efficiency, one might imagine a scenario in which proteins evolve positively charged amino acid substitutions within MADs previously lacking such charges so that dual localization to cytosol and to intracellular membranes can be simply achieved. Certainly, current prediction methods for MADs might be considered overly conservative, and further evidence of snorkeling should prompt the development of improved algorithms that consider positively charged amino acids to be acceptable within certain positions of a predicted MAD.

The membrane-associated domain of the Fis1p tail-anchor may consist of two separable segments

Computational analyses suggest that the Fis1p TA is mostly alpha-helical in nature (Buchan *et al.*, 2013; Drozdetskiy *et al.*, 2015). We found that proper localization of the

Fis1p TA likely requires its predicted alpha-helicity within the MAD, since proline, which is known to break or kink helices (Senes *et al.*, 2004), profoundly disrupts targeting when substituted at many positions throughout this hydrophobic region. However, we found that replacement by proline is more acceptable at a specific location, G137, than proline mutations found at previous or subsequent locations within this region, potentially indicating that the Fis1p MAD is bipartite in nature. Further supporting a bipartite structure of the Fis1p MAD, insertion of new amino acids between A135 and G136 did not apparently affect mitochondrial TA targeting. Moreover, mutations toward the carboxyl-terminal end of the Fis1p MAD appear to affect mitochondrial targeting more drastically, as reported by deep mutational scanning, than mutations toward the amino terminus of the transmembrane segment. Previous analysis of the yeast Tom5p TA and rat OMP25 TA also support a bipartite structure of the MAD, with higher sensitivity to mutation nearer to the carboxyl-terminal end of this hydrophobic stretch (Horie *et al.*, 2002). In addition, prolines are found within the MAD of the mammalian OMb and OMP25 TAs, and a proline within the MAD of Tom5p has been demonstrated to be important for targeting to mitochondria (Allen *et al.*, 2002). These results suggest that those prolines might demarcate the boundary between distinct structural regions of the targeting sequence. On the other hand, prolines within a single helical segment may simply be more easily housed within an alpha-helix when buried deep in the lipid bilayer (Li *et al.*, 1996; Senes *et al.*, 2004) and may not reflect two separable MAD segments. If this is the case, prolines found in mitochondrial TAs might indicate the portion of the TA found at the midpoint of the OM.

Glycine is not preferred within alpha-helices (Chou and Fasman, 1974; O'Neil and DeGrado, 1990) as a consequence of its conformational flexibility. However, our deep mutational scan does not indicate reduced membrane targeting when most amino acids within the Fis1p TA are individually mutated to glycine. This might be surprising in light of the pronounced effects provided by several proline replacement mutations throughout this domain. However, glycine may not be as disruptive for alpha-helices found within a lipid bilayer environment when compared with alpha-helices of soluble

proteins, due to better intra-helical hydrogen bonding within the hydrophobic environment of the membrane (Dong *et al.*, 2012). Indeed, four glycines already exist within the *S. cerevisiae* Fis1p TA. The TAs of Fis1p orthologs are also littered with glycines (Stojanovski *et al.*, 2004), further indicating that glycines are less disruptive of the Fis1p TA than prolines. Interestingly, GXXXG motifs, and other similarly spaced small amino acids like alanine and serine, can promote helix packing within lipid bilayers (Russ and Engelman, 2000; Gimpelev *et al.*, 2004; Senes *et al.*, 2004). However, our findings demonstrate that the sole Fis1p GXXXG motif and a nearby AXXXA motif do not play a significant role in targeting of the Fis1p TA to membrane.

The Fis1p tail anchor may not be exposed to the intermembrane space

Four of five carboxyl-terminal residues of Fis1p are positively charged. Previous reports indicated that a positively charged carboxyl-terminus is important specifically for proper Fis1p targeting and generally for insertion of several other TAs at the mitochondrial OM (Isenmann *et al.*, 1998; Horie *et al.*, 2002; Habib *et al.*, 2003; Horie *et al.*, 2003; Yoon *et al.*, 2003; Stojanovski *et al.*, 2004). Further supporting the importance of this highly charged region, our genetic selection and subsequent microscopic analysis revealed that the last five amino acids within the Fis1p sequence are important for effective insertion, as indicated by our genetic assessment, and for membrane specificity, as indicated by our microscopic analysis. How this charged region promotes localization and insertion is not yet clear.

The currently accepted view of Fis1p topology is that this positively charged carboxyl-terminus is ultimately exposed to the mitochondrial intermembrane space. However, a presumably high energetic barrier (Parsegian, 1969; Engelman and Steitz, 1981; Honig and Hubbell, 1984) makes it difficult to countenance the transfer of the highly charged carboxyl-terminus of mitochondrial TA proteins across a lipid bilayer without the assistance of an aqueous pore. Interestingly, organellar import of mitochondrial TA-containing proteins appears saturable in mammalian cells (Setoguchi *et al.*, 2006),

potentially indicating a finite number of translocons capable of transporting mitochondrial TAs. Furthermore, the TOM complex has been reported to assist in insertion of full-length BAX into mitochondria (Ott *et al.*, 2007; Cartron *et al.*, 2008; Colin *et al.*, 2009). Potentially consistent with the need for a mitochondrial TA translocation machinery, the hFIS1 TA localizes specifically to mitochondria in human cells (Suzuki *et al.*, 2003), but cannot effectively localize mCherry to *S. cerevisiae* mitochondria, possibly suggesting evolutionary divergence and a structural mismatch between the hFIS1 TA and the putative yeast TA translocation apparatus. However, we note that not all human mitochondrial TAs fail to be imported at the proper organelle in yeast, since our genetic and microscopic results indicate that the human BAX TA is properly inserted into yeast mitochondria.

Other evidence supports the idea that mitochondrial tail-anchored proteins like Fis1p do not require a translocation machinery and can spontaneously insert into the OM. First, the MAD of the TA is protected from chemical modification upon exposure to lipid vesicles devoid of protein (Kemper *et al.*, 2008), suggesting that the Fis1p TA can insert into lipid bilayers without assistance. Moreover, blockade or destruction of the general insertion pore for mitochondrial proteins, associated receptors, or other outer membrane protein biogenesis machinery such as the SAM complex or the MIM complex did not prevent Fis1p insertion at yeast mitochondria (Stojanovski *et al.*, 2007; Kemper *et al.*, 2008; Sinzel *et al.*, 2016). Tail-anchored proteins also appear to have the ability to spontaneously and rapidly insert into mammalian mitochondria without the need for the TOM complex or soluble cytosolic chaperones (Setoguchi *et al.*, 2006), although cytosolic factors likely play a role in maintaining solubility stability of tail-anchored proteins while they are *en route* to mitochondria (Itakura *et al.*, 2016). Further supporting the absence of a translocation machinery dedicated to TA insertion, a large-scale screen for proteins required for proper localization of mitochondrial tail-anchored proteins uncovered no putative translocon components (Krumpe *et al.*, 2012). Finally, although not evaluated in this work due to strong repression of peroxisome biogenesis under the culture conditions utilized (Einerhand *et al.*, 1991; Van der Leij *et al.*, 1993), a

small fraction of cellular Fis1p may function at peroxisomes to mediate peroxisomal fission (Koch *et al.*, 2005; Kuravi *et al.*, 2006). A machinery that allows Fis1p TA insertion would potentially be shared by both mitochondria and peroxisomes, but no dual-localized translocation machinery has yet been identified.

How can one reconcile abundant evidence for spontaneous insertion of TAs into the mitochondrial OM with the presence of a highly charged region at the carboxyl-terminus of the Fis1p TA that has been assumed to be translocated? We suggest the possibility that while the Fis1p TA is inserted into the mitochondrial OM, it does not reach through to the intermembrane space. Rather, the Fis1p TA may be mostly buried within the outer leaflet of the OM, making transit of the positively charged terminus through the lipid bilayer unnecessary. Such a scenario is supported by studies suggesting that the TA of BAX is constantly inserted into the mitochondrial OM in non-apoptotic cells, then removed from the mitochondrial surface and returned to the cytosol (Edlich *et al.*, 2011; Schellenberg *et al.*, 2013). Constitutive extraction of BAX that has completely passed through the OM and exposes polypeptide to the intermembrane space seems unnecessarily expensive from an energetic standpoint. Rather, it is conceivable that the TA of inactive BAX is monotopically integrated within the plane of the membrane, thereby facilitating recycling. If true, Fis1p may take on a similar topology due to structural similarity between the BAX and Fis1p TAs. Moreover, the snorkeling of lysine or arginine placed into the Fis1p TA that is suggested by findings reported here is consistent with both bitopic and monotopic insertion (Strandberg and Killian, 2003). A caveat regarding any model in which Fis1p is monotopic at the OM is that neither the WT Fis1p TA nor any functional TA charge mutants produced in this study are characterized by the predicted amphiphilicity that is thought to promote oblique insertion at membranes (Sapay *et al.*, 2006). We would like to note that some form of membrane insertion is likely important for Fis1p functionality; our preliminary studies suggest that replacement of the TA in Fis1p with a domain from the Num1 protein that promotes peripheral association with the mitochondrial outer

membrane (Ping *et al.*, 2016) did not allow for mitochondrial division (A. Keskin, unpublished results).

Computational modeling informed by our high-throughput dataset, as well as further experimental work, will allow testing of whether Fis1p is monotopic or truly passes through the mitochondrial OM. Moreover, if a TA insertion machinery does exist at the mitochondrial OM, loss-of-function mutations affecting this machinery would presumably be recovered by the application of our genetic selection scheme. Finally, refined analysis of other organelle targeting signals and membrane insertion sequences can be accomplished by applying the deep mutational scanning approach outlined in this study.

MATERIALS AND METHODS:

Yeast strains and plasmids

Details of strains used in this study are provided in Table S2. Plasmid acquisition details and associated references, as well as details of plasmid construction, are found in Table S3. Oligonucleotides used in this study are listed in Table S4.

Culture conditions

Synthetic complete (SC) medium contains 0.67% yeast nitrogen base without amino acids, 2% dextrose, 0.1% casamino acids, 50 µg/ml adenine hemisulfate, and either 25 µg/ml uracil (SC-Trp) or 100 µg/ml L-tryptophan (SC-Ura). Supplemented minimal medium (SMM) contains 0.67% yeast nitrogen base without amino acids, 2% dextrose, 20 µg/ml adenine hemisulfate, 20 µg/ml uracil, 20µg/ml methionine, 30 µg/ml lysine. SMM also contains, depending on selection needs, 20 µg/ml histidine, 100 µg/ml leucine, and/or 20 µg/ml tryptophan, as indicated. SLac medium lacking histidine contains 0.67% yeast nitrogen base without amino acids, 1.2% NaOH, a volume of lactic acid sufficient to subsequently bring the pH to 5.5, 20 µg/ml adenine hemisulfate, 20 µg/ml uracil, 20 µg/ml methionine, 30 µg/ml lysine, 100 µg/ml leucine, and 20 µg/ml tryptophan. Solid media also contain 1.7% bacteriological agar. Cells were incubated at 30˚C unless otherwise indicated. For serial dilution assays, strains in logarithmic proliferation phase were diluted to an OD_{600} of 0.1, and 4 µL of this dilution and three serial five-fold dilutions were spotted to solid medium.

Assessment of Fis1p function using a mtDNA loss assay

Cells lose mtDNA and the ability to proliferate on non-fermentable medium when mitochondrial fusion is blocked unless mitochondria division is also abrogated (Sesaki and Jensen, 1999; Fekkes *et al.*, 2000; Mozdy *et al.*, 2000; Tieu and Nunnari, 2000).

Strain CDD688 (Mutlu *et al.*, 2014) harbors chromosomal deletions in *FZO1* and *FIS1* and a CHX-counterselectable plasmid expressing *FZO1*. Upon removal of plasmid-expressed *FZO1*, cells will maintain mtDNA and respire unless functional *FIS1* allowing mitochondrial division is also present. To assess the functionality of Fis1p variants containing TA mutations, strain CDD688 was transformed with plasmids expressing WT *FIS1* or variants mutated within the Fis1p TA. Transformants were cultured overnight in SMM-His medium lacking CHX to permit cells to lose the *FZO1*-encoding plasmid. Serial dilutions were then spotted to SLac-His+3 µg/mL CHX ("lactate / no fusion") and incubated for 5 d to test for maintenance of mtDNA following counterselection for *FZO1*, with cell proliferation indicating a lack of Fis1p function. As a control for cell proliferation under conditions not selective for mtDNA maintenance, an equal number of cells was also spotted to SMM-Trp-His medium ("glucose / fusion") and incubated for 2 d.

Microscopy

For epifluorescence microscopy, cells in the logarithmic phase of proliferation were examined using an Eclipse 80i microscope with a 100X Plan Fluor objective and linked to a DS-Qi1Mc camera (Nikon, Tokyo, Japan). Cells were cultured in SMM medium appropriate for plasmid selection. Exposure times were automatically determined, and images were captured using NIS-Elements version AR 3.2. All images of mCherry expression were brightness adjusted in Adobe Photoshop CS5 (Adobe, San Jose, California) to an equivalent extent, except when the mCherry-BAX(TA) signal was assessed. For presentation of data associated with this fusion protein, the 'autolevels' adjustment was used. Scoring of mitochondrial morphology was performed blind to genotype. To promote mitochondrial fragmentation, sodium azide was added at a concentration of 500 µM for 60 min before fluorescence microscopy. For staining of mitochondrial nucleoids, 4'6-diamidino-2-phenylindole (DAPI) was added to cultures at a concentration of 1 µg/ml and cells were incubated for 15 min before analysis.

717 *Fis1p TA mutant library construction*

718

719 Recombination-based cloning (Oldenburg *et al.*, 1997) was used to generate
720 constructs expressing Gal4-Fis1p and mutated at one of 27 positions within the Fis1p
721 TA. Two DNA segments generated by PCR were fused in this recombination reaction.
722 The 5' portion was amplified by PCR from template plasmid b100 using primer 698 and
723 the appropriate primer (rvsposX) listed in Table S4. The 3' section was generated from
724 template b100 using primers 517 and the relevant primer (fwdposX) listed in Table S4.
725 PCR products were recombined into *Not*I-linearized pKS1 by co-transformation of
726 vector and PCR products into strain MaV203. Each sub-library for each Fis1p TA
727 position was generated individually by selection of Trp^+ clones in liquid medium, with a
728 portion of each transformation reaction plated to solid SC-Trp medium to confirm
729 recombination and transformation efficiency. To generate the total pool prior to
730 selection for Gal4p-mediated transcription, equal numbers of cells, as determined by
731 OD_{600} measurement, were taken from overnight cultures of each sub-library and
732 combined within the same liquid culture. Note that all constructs expressing Gal4-
733 Fis1p also contain superfolder GFP (Pédelacq *et al.*, 2005)(REF) in frame between the
734 Gal4p and Fis1p segments, but for simplicity, this is typically omitted from figure labels
735 and from the text.

736

737

Deep mutational scanning of the Fis1p TA library

The pool of constructs containing Fis1p TA mutations was cultured for four generations in SC-Trp medium, SC-Ura medium, or SMM-Trp-His medium containing 0 mM, 5 mM, 10 mM, or 20 mM 3-AT. Plasmids present under each culture condition were then harvested from 10 OD_{600} units of cells. To harvest each plasmid library, cells were pelleted at 4,000g for 3 min, then washed with 5 ml 0.9 M D-sorbitol and resuspended in 1 ml of 0.9 M D-sorbitol. One "stick-full" of zymolyase 20T (Amsbio, Abingdon, United Kingdom), was added, and cells were incubated at 37˚C for 45 min. Cells were again collected at 4,000g for 3 min and processed using a plasmid purification kit (GeneJET Plasmid Miniprep Kit, Thermo Scientific, Waltham, USA) using the manufacturer's instructions. Primers 882 and 883 were used to amplify the genomic region encoding the Fis1p TA from each plasmid pool. Using the provided PCR products, next-generation, paired-end sequencing was performed by Microsynth (Balgach, Switzerland) on a MiSeq Nano (2x150v2). The resulting FASTQ output can be found at [to be uploaded to Dryad Digital Repository and link provided, article acceptance required for upload]. FASTQ output from paired ends and lacking adaptor sequences was combined into a single segment using the PANDAseq assembler version 2.8 (Masella *et al.*, 2012). The TRIM function (trimmer Galaxy tool version 0.0.1) was performed using the resources of the Galaxy Project (Goecks *et al.*, 2010) in order to remove sequences not directly encoding the defined Fis1p and stop codon. Further processing in Microsoft Excel (Redmond, USA) subsequently allowed conversion of DNA sequence to amino acid sequence and removal of those TAs with more than one amino acid mutation from further analysis. Enrichment values reflect, at a given amino acid position, the ratio of the fraction of amino acid counts following selection to the fraction of amino acid counts in the starting library. Enrichment values are not derived through comparisons across different amino acid positions. Counts for the native amino acid at each position were set as the total number of TA counts for which all amino acids were WT within a given selected pool. When calculating enrichment values, TA amino acid replacements for which there were zero reads in the SC-Trp

768 sample had their value changed to one in order to allow possible detection of
769 enrichment under selective conditions by preventing division by zero. Heat maps were
770 generated using the Matrix2png utility (Pavlidis and Noble, 2003).

ACKNOWLEDGEMENTS:

We thank Gülayşe İnce Dunn, Bengisu Seferoğlu, Güleycan Bal, Funda Kar, and Sara Nafisi for comments on this manuscript. This work was supported by a European Research Council Starting Grant (637649-RevMito) to CDD, by a European Molecular Biology Organization Installation Grant (2138) to CDD, and by Koç University.

CONFLICT OF INTEREST STATEMENT:

The authors have no known conflict of interest affecting the outcome or interpretation of this study.

FIGURE LEGENDS:

Figure 1. A genetic selection based on protein mislocalization allows recovery of mutations blocking Fis1p TA localization to mitochondria. (A) A scheme for selection of mutations preventing mitochondrial targeting of the Fis1p TA. Full-length Fis1p is fused to the transcription factor Gal4p (and to superfolder GFP, not shown). Upon failure to localize Fis1p at the mitochondrial OM, Gal4p is free to translocate to the nucleus and activate *HIS3* and *URA3*. (B) Removal of the Fis1p TA allows proliferation on medium requiring *HIS3* activation or *URA3* activation. Strain MaV203 expressing Gal4-Fis1p variants from plasmids b100 (WT), b101 (ΔTA), or harboring empty vector pKS1 was cultured in SC-Trp medium, then, following serial dilution, spotted to SC-Trp, SMM-His + 20 mM 3-AT, or SC-Ura and incubated for 2 d.

Figure 2. Selection for reporter activation by Gal4-Fis1p reveals TA mutations required for full mitochondrial localization. (A) Missense mutations within the Fis1p TA provide selectable marker activation. Strain MaV203 expressing Gal4-Fis1p variants from plasmids b100 (WT), b128 (V145E), b129 (L139P), b130 (L129P, V138A), or b101 (ΔTA) were treated as in Figure 1B. (B) Missense mutations within the Fis1p TA allow cytosolic accumulation of a linked mCherry protein. mCherry fused to variants of the Fis1p TA were expressed in WT strain CDD961 from plasmids b109 (WT), b134 (V145E), b135 (L139P), b136 (L129P,V138A), or b252 (ΔTA) and visualized by fluorescence microscopy. Mitochondria were labelled with a mitochondria-targeted GFP expressed from plasmid pHS1. Scale bar, 5 μm.

Figure 3. Mutations within the TA of a Gal4-Fis1 fusion protein allow Gal4-driven transcription. The $\log_2$ of enrichment values for each amino acid were calculated for each position following selection in SMM-Trp-His medium containing 20 mM 3-AT. Enrichment values are generated for individual amino acid positions within the TA, and not across positions. Black outlines denote the native amino acid for each position.

Amino acid replacements not detectable under selective conditions are denoted by black, filled squares. The predicted MAD is indicated by a red line.

Figure 4. Identification of abundant Gal4-Fis1p clones which are highly enriched upon selection for Gal4-Fis1p nuclear translocation. (A) TA replacement mutations are plotted, with $\log_2$ enrichment values provided on the X-axis and sequence counts recovered from the starting pool (SC-Trp) provided on the Y-axis. Those replacement mutations that are within the top 75th percentile of mutant abundance in the starting pool and enriched at least four-fold following selection in SMM-Trp-His medium containing 20 mM 3-AT are highlighted in a blue box. (B) Expansion of the highlighted region in (A) showing specific TA mutations.

Figure 5. Proline substitution is acceptable at a discrete position within the Fis1p TA. (A) Replacement of specific amino acids within the TA of Gal4-Fis1p with proline can lead to Gal4-mediated selectable marker activation. Strain MaV203 expressing Gal4-Fis1p variants from plasmids b100 (WT), b188 (V134P), b189 (G137P), b129 (L139P), b190 (A140P), b296 (A144P), or b101 (ΔTA) was cultured in SC-Trp medium then spotted to SC-Trp or SMM-His + 20 mM 3-AT medium for 2 d. (B) TAs with specific proline replacements can reduce mitochondrial targeting of a linked fluorescent protein. Variants of the Fis1p TA fused to mCherry were expressed in WT strain CDD961 from plasmids b109 (WT), b208 (V134P), b209 (G137P), b135 (L139P), b210 (A140P), b211 (A144P) and examined, along with mitochondria-targeted GFP, as in Figure 2B. (C) Deletion of the Msp1p extractase does not allow tail-anchored proteins mistargeted due to proline inclusion to return to mitochondria. Cells from *msp1Δ/msp1Δ* strain CDD1044 expressing pHS1 and plasmids b109 (WT), b208 (V134P), b135 (L139P), b210 (A140P), or b211 (A144P) were inspected as in Figure 2B. Scale bar, 5 μm.

Figure 6. Targeting of the Fis1p TA is not dependent upon a specific TA length. (A) Deletion of up to three amino acids or insertion of up to three amino acids does not

allow Gal4-Fis1p to activate transcription. Mav203 cells expressing Gal4-Fis1p variants from plasmids b229 (∇1A), b230 (∇2A), b231 (∇3A), b226 (ΔG136), b227 (ΔA135-G136), b228 (ΔA135-G137), or b101 (ΔTA) were treated as in Figure 5A. (B) mCherry fused to a Fis1p TA containing an insertion of up to three amino acids in length localizes properly to mitochondria. Strain CDD961 expressing mCherry-TA fusions from plasmids b109 (WT), b235 (∇1A), b236 (∇2A), or b237 (∇3A) was visualized as in Figure 2B. (C) mCherry fused to a Fis1p TA deleted of up to three amino acids is properly targeted to mitochondria. Strain CDD961 expressing mCherry-TA fusions from plasmids b109 (WT), b232 (ΔG136), b233 (ΔA135-G136), or b234 (ΔA135-G137) was examined as in Figure 2B. Scale bar, 5 μm.

Figure 7. The positively charged carboxyl-terminus of the Fis1p TA is important for specific localization to the mitochondrial outer membrane. (A) Deletion of the final five amino acids from the Fis1p TA permits transcriptional activation by Gal4-Fis1p. Strain Mav203 harboring plasmids b100 (WT), b253 (R151X), or b101 (ΔTA) was treated as in Figure 5A. (B) Removal of the last five amino acids from the Fis1p TA allows mislocalization to the secretory system. Strain CDD961 expressing mCherry fused to the WT Fis1p TA (b109) or expressing mCherry linked to a truncated Fis1p TA (R151X) from plasmid b254 was evaluated as in Figure 2B. White arrowheads denote mCherry localized to the nuclear envelope. Scale bar, 5 μm.

Figure 8. Negative charges allow higher transcriptional activity than positive charges when placed at specific positions within the Gal4-Fis1p TA. Strain MaV203 was transformed with plasmids pKS1 (vector), b100 (Gal4-Fis1), b101 [Gal4-Fis1(ΔTA)], or plasmids encoding the indicated charge replacements within the Fis1p TA (plasmids b173-b187 and b295). The resulting transformants were treated as in Figure 5A.

Figure 9. Fis1p TA targeting is hindered to a greater extent by inclusion of negatively charged amino acids than by positively charged amino acids. (A) Examination of mCherry-TA localization in WT cells expressing Msp1p. Strain CDD961 was

transformed with plasmids (b192-b207) expressing mCherry linked to the Fis1p TA harboring the indicated substitutions. Cells were visualized as in Figure 2B. (B) Deletion of Msp1p does not allow recovery of mitochondrial localization by poorly targeted mCherry-TA variants. Strain CDD1044, deleted of Msp1p, was transformed with the following plasmids encoding mCherry fused to the mutant TAs: b192 (V132D), b196 (A140D), b197 (A140E), b198 (A140K), b199 (A140R), b200 (A144D), b201 (A144E), b134 (V145E), b204 (F148D), b205 (F148E). Transformants were examined as in Figure 2B. Scale bar, 5 μm.

Figure 10. Positive and negative charge replacements within the Fis1p TA can generally support Fis1p function. (A) Normal mitochondrial morphology can be maintained even when charges are placed within the hydrophobic MAD of the Fis1p TA. Strain CDD741 was transformed with vector pRS313, a plasmid expressing WT Fis1p (b239), or plasmids expressing Fis1p containing the indicated TA alterations (plasmids b240-251). Mitochondrial morphology was visualized by expression of mitochondria-targeted GFP from plasmid pHS12. Scale bar, 5 μm. (B) Induced, Fis1p-dependent mitochondrial fragmentation is permitted by charge placement within the Fis1p TA. Transformants analyzed in (A) were treated with sodium azide to provoke mitochondrial fragmentation, and cells were scored for the maintenance of a mitochondrial network (n=200 cells). (C) Charged residues within the TA provide exhibit Fis1p activity during a genetic assay of Fis1p function. *fzo1Δ fis1Δ* strain CDD688, carrying a CHX-counterselectable, *FZO1*-expressing plasmid, was transformed with the *FIS1*-expressing plasmids enumerated above. After allowing cells to lose the *FZO1*-encoding plasmid, serial dilutions were spotted to SLac-His containing 3 μg/mL CHX to counterselect against *FZO1* expression ("lactate / no fusion") and incubated for 5 d to test for maintenance of mtDNA. Cell proliferation indicates a lack of Fis1p activity. To control for cell number spotted, cells from the same culture were placed on SMM-Trp-His medium ("glucose / fusion") and incubated for 2 d.

REFERENCES:

Allen, R., Egan, B., Gabriel, K., Beilharz, T., and Lithgow, T. (2002). A conserved proline residue is present in the transmembrane-spanning domain of Tom7 and other tail-anchored protein subunits of the TOM translocase. FEBS Lett *514*, 347–350.

Araya, C. L., and Fowler, D. M. (2011). Deep mutational scanning: assessingprotein function on a massive scale. Trends in Biotechnology *29*, 435–442.

Beilharz, T. (2003). Bipartite Signals Mediate Subcellular Targeting of Tail-anchored Membrane Proteins in Saccharomyces cerevisiae. *278*, 8219–8223.

Borgese, N., Brambillasca, S., and Colombo, S. (2007). How tails guide tail-anchored proteins to their destinations. Current Opinion in Cell Biology *19*, 368–375.

Borgese, N., Gazzoni, I., Barberi, M., Colombo, S., and Pedrazzini, E. (2001). Targeting of a tail-anchored protein to endoplasmic reticulum and mitochondrial outer membrane by independent but competing pathways. Mol Biol Cell *12*, 2482–2496.

Boucher, J. I., Cote, P., Flynn, J., Jiang, L., Laban, A., Mishra, P., Roscoe, B. P., and Bolon, D. N. A. (2014). Viewing protein fitness landscapes through a next-gen lens. Genetics *198*, 461–471.

Buchan, D. W. A., Minneci, F., Nugent, T. C. O., Bryson, K., and Jones, D. T. (2013). Scalable web services for the PSIPRED Protein Analysis Workbench. Nucleic Acids Res *41*, W349–W357.

Cartron, P.-F., Bellot, G., Oliver, L., Grandier-Vazeille, X., Manon, S., and Vallette, F. M. (2008). Bax inserts into the mitochondrial outer membrane by different mechanisms. FEBS Lett *582*, 3045–3051.

Chen, Y.-C., Umanah, G. K. E., Dephoure, N., Andrabi, S. A., Gygi, S. P., Dawson, T. M., Dawson, V. L., and Rutter, J. (2014). Msp1/ATAD1 maintains mitochondrial function by facilitating the degradation of mislocalized tail-anchored proteins. Embo J *33*, 1548–1564.

Chou, P. Y., and Fasman, G. D. (1974). Conformational parameters for amino acids in helical, beta-sheet, and random coil regions calculated from proteins. Biochemistry *13*, 211–222.

Colin, J., Garibal, J., Mignotte, B., and Guenal, I. (2009). The mitochondrial TOM complex modulates bax-induced apoptosis in Drosophila. Biochemical and Biophysical Research Communications *379*, 939–943.

Cymer, F., Heijne, von, G., and White, S. H. (2015). Mechanisms of Integral Membrane Protein Insertion and Folding. J Mol Biol *427*, 999–1022.

de Mendoza, D., and Cronan, J. E., Jr. (1983). Thermal regulation of membrane lipid fluidity in bacteria. Trends in Biochemical Sciences *8*, 49–52.

Denic, V., Dötsch, V., and Sinning, I. (2013). Endoplasmic reticulum targeting and insertion of tail-anchored membrane proteins by the GET pathway. Cold Spring Harbor Perspectives in Biology *5*, a013334–a013334.

Deshaies, R. J., and Schekman, R. (1987). A yeast mutant defective at an early stage in import of secretory protein precursors into the endoplasmic reticulum. J Cell Biol *105*, 633–645.

Dong, H., Sharma, M., Zhou, H.-X., and Cross, T. A. (2012). Glycines: Role in α-Helical Membrane Protein Structures and a Potential Indicator of Native Conformation. Biochemistry *51*, 4779–4789.

Drozdetskiy, A., Cole, C., Procter, J., and Barton, G. J. (2015). JPred4: a protein secondary structure prediction server. Nucleic Acids Res *43*, W389–W394.

Dufourc, E. J. (2008). Sterols and membrane dynamics. J Chem Biol *1*, 63–77.

Dunn, C. D., and Jensen, R. E. (2003). Suppression of a defect in mitochondrial protein import identifies cytosolic proteins required for viability of yeast cells lacking mitochondrial DNA. Genetics *165*, 35–45.

Durfee, T., Becherer, K., Chen, P. L., Yeh, S. H., Yang, Y., Kilburn, A. E., Lee, W. H., and Elledge, S. J. (1993). The retinoblastoma protein associates with the protein phosphatase type 1 catalytic subunit. Genes Dev *7*, 555–569.

Edlich, F., Banerjee, S., Suzuki, M., Cleland, M. M., Arnoult, D., Wang, C., Neutzner, A., Tjandra, N., and Youle, R. J. (2011). Bcl-xL Retrotranslocates Bax from the Mitochondria into the Cytosol. Cell *145*, 104–116.

Einerhand, A. W., Voorn-Brouwer, T. M., Erdmann, R., Kunau, W. H., and Tabak, H. F. (1991). Regulation of transcription of the gene coding for peroxisomal 3-oxoacyl-CoA thiolase of Saccharomcyes cerevisiae. European Journal of Biochemistry *200*, 113–122.

Elazar, A., Weinstein, J., Biran, I., Fridman, Y., Bibi, E., and Fleishman, S. J. (2016). Mutational scanning reveals the determinants of protein insertion and association energetics in the plasma membrane. eLife *5*, 1302.

Engelman, D. M., and Steitz, T. A. (1981). The spontaneous insertion of proteins into and across membranes: the helical hairpin hypothesis. Cell *23*, 411–422.

Fekkes, P., Shepard, K. A., and Yaffe, M. P. (2000). Gag3p, an outer membrane protein required for fission of mitochondrial tubules. J Cell Biol *151*, 333–340.

969 Fowler, D. M., and Fields, S. (2014). Deep mutational scanning: a new style of protein
970 science. Nature Publishing Group *11*, 801–807.

971 Förtsch, J., Hummel, E., Krist, M., and Westermann, B. (2011). The myosin-related
972 motor protein Myo2 is an essential mediator of bud-directed mitochondrial movement
973 in yeast. J Cell Biol *194*, 473–488.

974 Garipler, G., Mutlu, N., Lack, N. A., and Dunn, C. D. (2014). Deletion of conserved
975 protein phosphatases reverses defects associated with mitochondrial DNA damage in
976 Saccharomyces cerevisiae. Proceedings of the National Academy of Sciences *111*,
977 1473–1478.

978 Gimpelev, M., Forrest, L. R., Murray, D., and Honig, B. (2004). Helical Packing Patterns
979 in Membrane and Soluble Proteins. Biophysical Journal *87*, 4075–4086.

980 Goecks, J., Nekrutenko, A., Taylor, J., Galaxy Team (2010). Galaxy: a comprehensive
981 approach for supporting accessible, reproducible, and transparent computational
982 research in the life sciences. Genome Biol *11*, R86.

983 Gross, A., Pilcher, K., Blachly-Dyson, E., Basso, E., Jockel, J., Bassik, M. C.,
984 Korsmeyer, S. J., and Forte, M. (2000). Biochemical and Genetic Analysis of the
985 Mitochondrial Response of Yeast to BAX and BCL-XL. Mol Cell Biol *20*, 3125–3136.

986 Habib, S. J., Vasiljev, A., Neupert, W., and Rapaport, D. (2003). Multiple functions of
987 tail-anchor domains of mitochondrial outer membrane proteins. FEBS Lett *555*, 511–
988 515.

989 He, S., and Fox, T. D. (1999). Mutations affecting a yeast mitochondrial inner
990 membrane protein, pnt1p, block export of a mitochondrially synthesized fusion protein
991 from the matrix. Mol Cell Biol *19*, 6598–6607.

992 Hermann, G. J., Thatcher, J. W., Mills, J. P., Hales, K. G., Fuller, M. T., Nunnari, J., and
993 Shaw, J. M. (1998). Mitochondrial fusion in yeast requires the transmembrane GTPase
994 Fzo1p. J Cell Biol *143*, 359–373.

995 Hietpas, R. T., Jensen, J. D., and Bolon, D. N. A. (2011). Experimental illumination of a
996 fitness landscape. Proceedings of the National Academy of Sciences *108*, 7896–7901.

997 Honig, B. H., and Hubbell, W. L. (1984). Stability of “salt bridges” in membrane
998 proteins. Proc Natl Acad Sci USA *81*, 5412–5416.

999 Horie, C., Suzuki, H., Sakaguchi, M., and Mihara, K. (2002). Characterization of signal
1000 that directs C-tail-anchored proteins to mammalian mitochondrial outer membrane.
1001 Mol Biol Cell *13*, 1615–1625.

1002 Horie, C., Suzuki, H., Sakaguchi, M., and Mihara, K. (2003). Targeting and assembly of
1003 mitochondrial tail-anchored protein Tom5 to the TOM complex depend on a signal

distinct from that of tail-anchored proteins dispersed in the membrane. J Biol Chem *278*, 41462–41471.

Isenmann, S., Khew-Goodall, Y., Gamble, J., Vadas, M., and Wattenberg, B. W. (1998). A splice-isoform of vesicle-associated membrane protein-1 (VAMP-1) contains a mitochondrial targeting signal. Mol Biol Cell *9*, 1649–1660.

Itakura, E., Zavodszky, E., Shao, S., Wohlever, M. L., Keenan, R. J., and Hegde, R. S. (2016). Ubiquilins Chaperone and Triage Mitochondrial Membrane Proteins for Degradation. Molecular Cell, 1–14.

Jensen, R. E., Schmidt, S., and Mark, R. J. (1992). Mutations in a 19-amino-acid hydrophobic region of the yeast cytochrome c1 presequence prevent sorting to the mitochondrial intermembrane space. Mol Cell Biol *12*, 4677–4686.

Johnson, N., Powis, K., and High, S. (2013). Post-translational translocation into the endoplasmic reticulum. BBA-Molecular Cell Research *1833*, 2403–2409.

Kemper, C., Habib, S. J., Engl, G., Heckmeyer, P., Dimmer, K. S., and Rapaport, D. (2008). Integration of tail-anchored proteins into the mitochondrial outer membrane does not require any known import components. Journal of Cell Science *121*, 1990–1998.

Kim, C., Schmidt, T., Cho, E.-G., Ye, F., Ulmer, T. S., and Ginsberg, M. H. (2012). Basic amino-acid side chains regulate transmembrane integrin signalling. Nature *481*, 209–213.

Klecker, T., Wemmer, M., Haag, M., Weig, A., Böckler, S., Langer, T., Nunnari, J., and Westermann, B. (2015). Interaction of MDM33 with mitochondrial inner membrane homeostasis pathways in yeast. Sci. Rep., 1–14.

Koch, A., Yoon, Y., Bonekamp, N. A., McNiven, M. A., and Schrader, M. (2005). A role for Fis1 in both mitochondrial and peroxisomal fission in mammalian cells. Mol Biol Cell *16*, 5077–5086.

Krumpe, K., Frumkin, I., Herzig, Y., Rimon, N., Özbalci, C., Brügger, B., Rapaport, D., and Schuldiner, M. (2012). Ergosterol content specifies targeting of tail-anchored proteins to mitochondrial outer membranes. Mol Biol Cell *23*, 3927–3935.

Kuravi, K., Nagotu, S., Krikken, A. M., Sjollema, K., Deckers, M., Erdmann, R., Veenhuis, M., and van der Klei, I. J. (2006). Dynamin-related proteins Vps1p and Dnm1p control peroxisome abundance in Saccharomyces cerevisiae. Journal of Cell Science *119*, 3994–4001.

Kuroda, R., Ikenoue, T., Honsho, M., Tsujimoto, S., Mitoma, J. Y., and Ito, A. (1998). Charged amino acids at the carboxyl-terminal portions determine the intracellular locations of two isoforms of cytochrome b5. J Biol Chem *273*, 31097–31102.

Lee, J., Kim, D. H., and Hwang, I. (2014). Specific targeting of proteins to outer envelope membranes of endosymbiotic organelles, chloroplasts, and mitochondria. Front Plant Sci *5*, 173.

Lee, S., Lim, W. A., and Thorn, K. S. (2013). Improved blue, green, and red fluorescent protein tagging vectors for S. cerevisiae. PLoS ONE *8*, e67902.

Li, S. C., Goto, N. K., Williams, K. A., and Deber, C. M. (1996). Alpha-helical, but not beta-sheet, propensity of proline is determined by peptide environment. Proc Natl Acad Sci USA *93*, 6676–6681.

Long, S. B., Campbell, E. B., and MacKinnon, R. (2005). Voltage Sensor of Kv1.2: Structural Basis of Electromechanical Coupling. Science *309*, 903–908.

Maarse, A. C., Blom, J., Grivell, L. A., and Meijer, M. (1992). MPI1, an essential gene encoding a mitochondrial membrane protein, is possibly involved in protein import into yeast mitochondria. Embo J *11*, 3619–3628.

Masella, A. P., Bartram, A. K., Truszkowski, J. M., Brown, D. G., and Neufeld, J. D. (2012). PANDAseq: paired-end assembler for illumina sequences. BMC Bioinformatics *13*, 31.

Melamed, D., Young, D. L., Gamble, C. E., Miller, C. R., and Fields, S. (2013). Deep mutational scanning of an RRM domain of the Saccharomyces cerevisiae poly(A)-binding protein. Rna *19*, 1537–1551.

Meyers, S., Schauer, W., Balzi, E., Wagner, M., Goffeau, A., and Golin, J. (1992). Interaction of the yeast pleiotropic drug resistance genes PDR1 and PDR5. Curr Genet *21*, 431–436.

Monné, M., Nilsson, I., Johansson, M., Elmhed, N., and Heijne, von, G. (1998). Positively and negatively charged residues have different effects on the position in the membrane of a model transmembrane helix. J Mol Biol *284*, 1177–1183.

Mozdy, A. D., McCaffery, J. M., and Shaw, J. M. (2000). Dnm1p GTPase-mediated mitochondrial fission is a multi-step process requiring the novel integral membrane component Fis1p. J Cell Biol *151*, 367–380.

Mutlu, N., Garipler, G., Akdoğan, E., and Dunn, C. D. (2014). Activation of the pleiotropic drug resistance pathway can promote mitochondrial DNA retention by fusion-defective mitochondria in Saccharomyces cerevisiae. G3 (Bethesda) *4*, 1247–1258.

Nechushtan, A., Smith, C. L., Hsu, Y. T., and Youle, R. J. (1999). Conformation of the Bax C-terminus regulates subcellular location and cell death. Embo J *18*, 2330–2341.

Neupert, W. (2015). A Perspective on Transport of Proteins into Mitochondria: A Myriad

of Open Questions. J Mol Biol *427*, 1135–1158.

O'Neil, K. T., and DeGrado, W. F. (1990). A thermodynamic scale for the helix-forming tendencies of the commonly occurring amino acids. Science *250*, 646–651.

Okreglak, V., and Walter, P. (2014). The conserved AAA-ATPase Msp1 confers organelle specificity to tail-anchored proteins. Proceedings of the National Academy of Sciences *111*, 8019–8024.

Oldenburg, K. R., Vo, K. T., Michaelis, S., and Paddon, C. (1997). Recombination-mediated PCR-directed plasmid construction in vivo in yeast. Nucleic Acids Res *25*, 451–452.

Ott, M., Norberg, E., Walter, K. M., Schreiner, P., Kemper, C., Rapaport, D., Zhivotovsky, B., and Orrenius, S. (2007). The mitochondrial TOM complex is required for tBid/Bax-induced cytochrome c release. J Biol Chem *282*, 27633–27639.

Parsegian, A. (1969). Energy of an ion crossing a low dielectric membrane: solutions to four relevant electrostatic problems. Nature *221*, 844–846.

Pavlidis, P., and Noble, W. S. (2003). Matrix2png: a utility for visualizing matrix data. Bioinformatics *19*, 295–296.

Pédelacq, J.-D., Cabantous, S., Tran, T., Terwilliger, T. C., and Waldo, G. S. (2005). Engineering and characterization of a superfolder green fluorescent protein. Nat Biotechnol *24*, 79–88.

Ping, H. A., Kraft, L. M., Chen, W., Nilles, A. E., and Lackner, L. L. (2016). Num1 anchors mitochondria to the plasma membrane via two domains with different lipid binding specificities. J Cell Biol *266*, jcb.201511021–12.

Prasad, R., and Goffeau, A. (2012). Yeast ATP-Binding Cassette Transporters Conferring Multidrug Resistance. Annu. Rev. Microbiol. *66*, 39–63.

Rapaport, D. (2003). Finding the right organelle. Targeting signals in mitochondrial outer-membrane proteins. EMBO Rep *4*, 948–952.

Rapaport, D., Brunner, M., Neupert, W., and Westermann, B. (1998). Fzo1p is a mitochondrial outer membrane protein essential for the biogenesis of functional mitochondria in Saccharomyces cerevisiae. J Biol Chem *273*, 20150–20155.

Robinson, J. S., Klionsky, D. J., Banta, L. M., and Emr, S. D. (1988). Protein sorting in Saccharomyces cerevisiae: isolation of mutants defective in the delivery and processing of multiple vacuolar hydrolases. Mol Cell Biol *8*, 4936–4948.

Russ, W. P., and Engelman, D. M. (2000). The GxxxG motif: A framework for transmembrane helix-helix association. J Mol Biol *296*, 911–919.

1109 Ryan, K. R., Leung, R. S., and Jensen, R. E. (1998). Characterization of the
1110 mitochondrial inner membrane translocase complex: the Tim23p hydrophobic domain
1111 interacts with Tim17p but not with other Tim23p molecules. Mol Cell Biol *18*, 178–187.

1112 Sapay, N., Guermeur, Y., and Deléage, G. (2006). BMC Bioinformatics. BMC
1113 Bioinformatics *7*, 255–11.

1114 Schellenberg, B. *et al.* (2013). Bax Exists in a Dynamic Equilibrium between the Cytosol
1115 and Mitochondria to Control Apoptotic Priming. Molecular Cell *49*, 959–971.

1116 Schinzel, A., Kaufmann, T., Schuler, M., Martinalbo, J., Grubb, D., and Borner, C.
1117 (2004). Conformational control of Bax localization and apoptotic activity by Pro168. J
1118 Cell Biol *164*, 1021–1032.

1119 Schow, E. V., Freites, J. A., Cheng, P., Bernsel, A., Heijne, von, G., White, S. H., and
1120 Tobias, D. J. (2010). Arginine in Membranes: The Connection Between Molecular
1121 Dynamics Simulations and Translocon-Mediated Insertion Experiments. J Membrane
1122 Biol *239*, 35–48.

1123 Schuldiner, M., Metz, J., Schmid, V., Denic, V., Rakwalska, M., Schmitt, H. D.,
1124 Schwappach, B., and Weissman, J. S. (2008). The GET Complex Mediates Insertion of
1125 Tail-Anchored Proteins into the ER Membrane. Cell *134*, 634–645.

1126 Segrest, J. P., De Loof, H., Dohlman, J. G., Brouillette, C. G., and Anantharamaiah, G.
1127 M. (1990). Amphipathic helix motif: Classes and properties. Proteins: Structure,
1128 Function, and Bioinformatics *8*, 103–117.

1129 Senes, A., Engel, D. E., and DeGrado, W. F. (2004). Folding of helical membrane
1130 proteins: the role of polar, GxxxG-like and proline motifs. Current Opinion in Structural
1131 Biology *14*, 465–479.

1132 Sesaki, H., and Jensen, R. E. (1999). Division versus fusion: Dnm1p and Fzo1p
1133 antagonistically regulate mitochondrial shape. J Cell Biol *147*, 699–706.

1134 Setoguchi, K., Otera, H., and Mihara, K. (2006). Cytosolic factor- and TOM-
1135 independent import of C-tail-anchored mitochondrial outer membrane proteins. Embo
1136 J *25*, 5635–5647.

1137 Sikorski, R. S., and Hieter, P. (1989). A system of shuttle vectors and yeast host strains
1138 designed for efficient manipulation of DNA in Saccharomyces cerevisiae. Genetics *122*,
1139 19–27.

1140 Sinzel, M., Tan, T., Wendling, P., Kalbacher, H., Özbalci, C., Chelius, X., Westermann,
1141 B., Brügger, B., Rapaport, D., and Dimmer, K. S. (2016). Mcp3 is a novel mitochondrial
1142 outer membrane protein that follows a unique IMP-dependent biogenesis pathway.
1143 EMBO Rep *17*, 965–981.

Starita, L. M., Young, D. L., Islam, M., Kitzman, J. O., Gullingsrud, J., Hause, R. J., Fowler, D. M., Parvin, J. D., Shendure, J., and Fields, S. (2015). Massively Parallel Functional Analysis of BRCA1 RING Domain Variants. Genetics *200*, 413–422.

Stirling, C. J., Rothblatt, J., Hosobuchi, M., Deshaies, R., and Schekman, R. (1992). Protein translocation mutants defective in the insertion of integral membrane proteins into the endoplasmic reticulum. Mol Biol Cell *3*, 129–142.

Stojanovski, D., Guiard, B., Kozjak-Pavlovic, V., Pfanner, N., and Meisinger, C. (2007). Alternative function for the mitochondrial SAM complex in biogenesis of alpha-helical TOM proteins. J Cell Biol *179*, 881–893.

Stojanovski, D., Koutsopoulos, O. S., Okamoto, K., and Ryan, M. T. (2004). Levels of human Fis1 at the mitochondrial outer membrane regulate mitochondrial morphology. Journal of Cell Science *117*, 1201–1210.

Strandberg, E., and Killian, J. A. (2003). Snorkeling of lysine side chains in transmembrane helices: how easy can it get? FEBS Lett *544*, 69–73.

Suzuki, M., Jeong, S. Y., Karbowski, M., Youle, R. J., and Tjandra, N. (2003). The solution structure of human mitochondria fission protein Fis1 reveals a novel TPR-like helix bundle. J Mol Biol *334*, 445–458.

Taxis, C., and Knop, M. (2006). System of centromeric, episomal, and integrative vectors based on drug resistance markers for Saccharomyces cerevisiae.

Tieu, Q., and Nunnari, J. (2000). Mdv1p is a WD repeat protein that interacts with the dynamin-related GTPase, Dnm1p, to trigger mitochondrial division. J Cell Biol *151*, 353–366.

Van der Leij, I., Franse, M. M., Elgersma, Y., Distel, B., and Tabak, H. F. (1993). PAS10 is a tetratricopeptide-repeat protein that is essential for the import of most matrix proteins into peroxisomes of Saccharomyces cerevisiae. Proc Natl Acad Sci USA *90*, 11782–11786.

Vidal, M., Brachmann, R. K., Fattaey, A., Harlow, E., and Boeke, J. D. (1996a). Reverse two-hybrid and one-hybrid systems to detect dissociation of protein-protein and DNA-protein interactions. Proc Natl Acad Sci USA *93*, 10315–10320.

Vidal, M., Braun, P., Chen, E., Boeke, J. D., and Harlow, E. (1996b). Genetic characterization of a mammalian protein-protein interaction domain by using a yeast reverse two-hybrid system. Proc Natl Acad Sci USA *93*, 10321–10326.

Voss, N. R., Gerstein, M., Steitz, T. A., and Moore, P. B. (2006). The Geometry of the Ribosomal Polypeptide Exit Tunnel. J Mol Biol *360*, 893–906.

Wattenberg, B. W., Clark, D., and Brock, S. (2007). An artificial mitochondrial tail

signal/anchor sequence confirms a requirement for moderate hydrophobicity for targeting. Biosci Rep *27*, 385–401.

Wattenberg, B., and Lithgow, T. (2001). Targeting of C-terminal (tail)-anchored proteins: understanding how cytoplasmic activities are anchored to intracellular membranes. Traffic *2*, 66–71.

Wells, R. C., and Hill, R. B. (2011). The cytosolic domain of Fis1 binds and reversibly clusters lipid vesicles. PLoS ONE *6*, e21384.

Yoon, Y., Krueger, E. W., Oswald, B. J., and McNiven, M. A. (2003). The mitochondrial protein hFis1 regulates mitochondrial fission in mammalian cells through an interaction with the dynamin-like protein DLP1. Mol Cell Biol *23*, 5409–5420.

Yu, C.-H., Dang, Y., Zhou, Z., Wu, C., Zhao, F., Sachs, M. S., and Liu, Y. (2015). Codon Usage Influences the Local Rate of Translation Elongation to Regulate Co-translational Protein Folding. Molecular Cell *59*, 744–754.

SUPPLEMENTAL FIGURE AND TABLE LEGENDS:

Figure S1. A Gal4-Fis1 fusion localizes to mitochondria. *fis1Δ* strain CDD692 was transformed with plasmid b102, expressing a Gal4-Fis1p construct also harboring a central sfGFP domain from a high-copy plasmid. Mitochondrial DNA of live cells was stained with DAPI to reveal mitochondrial location. -located DNA and visualized by fluorescence microscopy. Scale bar, 5 μm.

Figure S2. Fusion to the Fis1p TA constrains Pdr1p activity. Strain BY4743 was transformed with plasmid b158 [Pdr1-Fis1(TA) WT], b159 [Pdr1-Fis1(TA) V145E], b160 [Pdr1-249-Fis1(TA) WT], b165 [Pdr1-249-Fis1(TA) V145E], or empty vector pRS316. Cells were cultured in SC-Ura medium, then spotted to SC-Ura medium or SC-Ura medium containing 0.2 μg/ml CHX and incubated for 2 d.

Figure S3. An examination of amino acid replacement representation within the Fis1p TA library. The fraction of counts representing each amino acid replacement in the starting SC-Trp library (fObs) was compared to the fraction that would be expected based on randomized codon recovery (fExp). Native amino acids are represented by a black square with a blue dot. Amino acid replacements with no representation in the library are represented by empty black squares. The predicted MAD is indicated by a red line.

Figure S4. Amino acid replacement frequencies within the Fis1p TA suggest that assessing histidine auxotrophy in the presence of 3-AT may provide the most informative results regarding Gal4-Fis1p location. Quantification of replacement in SMM-Trp-His medium without 3-AT (A), containing 5 mM 3-AT (B), containing 10mM 3-AT (C), or in SC-Ura medium (D). In all panels, black outlines indicate the native amino acid at each position within the Fis1p TA. Amino acid replacements not detectable under selective conditions are denoted by black, filled squares. The predicted MAD is indicated by a red line.

Figure S5. Little evidence exists for codon-level control of Gal4-Fis1p TA targeting. The $\log_2$ of enrichment values for each codon following selection of the Fis1p TA library in SMM-Trp-His medium containing 20 mM 3-AT are illustrated. Green outlines denote the native amino acid at each position. Codon replacements with no representation in the library following selection are represented by empty black squares. The predicted MAD is indicated by a red line.

Figure S6. Uracil auxotrophy tests that were performed alongside histidine auxotrophy tests. Samples cultured in SC-Trp for (A) Figure 5A, (B) Figure 6A, (C) Figure 7A, and (D) Figure 8 were also spotted to SC-Ura medium and incubated for 2 d.

Figure S7. mCherry fused to Fis1p TAs of varying length remains targeted to the ER in *spf1Δ* mutant cells. (A) Strain CDD1031, lacking Spf1p and expressing mCherry-TA fusions from plasmids b109 (WT), b235 (∇1A), b236 (∇2A), or b237 (∇3A), b232 (ΔG136), b233 (ΔA135-G136), or b234 (ΔA135-G137) were examined as in Figure 2B. White arrowheads denote mCherry localized to the nuclear envelope. Scale bar, 5 μm.

Figure S8. A mutated Fis1p TA lacking the positively charged carboxyl-terminus localizes to the ER independent of Get3p expression. *get3Δ/get3Δ* strain CDD1033 expressing mCherry fused to a WT Fis1p TA from plasmid b109 or expressing mCherry fused to a Fis1p TA lacking the positively charged carboxyl-terminus (R151X) from plasmid b254 were examined as in Figure 2B. Mitochondria were labelled with GFP expressed from pHS1. White arrowheads denote mCherry localized to the nuclear envelope. Scale bar, 5 μm.

Figure S9. The TAs of human proteins do not universally target to mitochondria in yeast. (A) The hFIS1 TA is mistargeted to the ER in *S. cerevisiae*. Strain CDD961 containing plasmid b257 expressing mCherry fused to the hFIS1 TA was analyzed as in

Figure 2B. (B) The hFIS1 TA does not permit activity of a fused Gal4p within the nucleus. Strain MaV203 was transformed with plasmid b100 (Gal4-Fis1), b258 [Gal4-hFIS1(TA)], or plasmid b101 (Gal4-Fis1ΔTA) and assessed as in Figure 5A. (C) The BAX TA can target to mitochondria in *S. cerevisiae*. Strain CDD961 transformed with plasmid b255, which expresses mCherry fused to the BAX TA, was examined as in Figure 2B. Scale bar, 5 μm.

Figure S10. Temperature affects the outcome of adding a positive charge to the Fis1p TA. Samples used in Figure 8 were also spotted to SMM-His medium containing 20 mM 3-AT and incubated at 18˚C for 4 d (A) or 37˚C for 3 d (B).

Figure S11. Most charge replacements within the Fis1p MAD permit Fis1p-dependent mitochondrial fragmentation. Images of azide-treated cells examined in Figure 10B are provided. Scale bar, 5 μm.

Table S1. Tail anchor sequence counts from individual pools.

Table S2. Strains used during this study.

Table S3. Plasmids used for experiments during this study.

Table S4. Oligonucleotides used in this study.

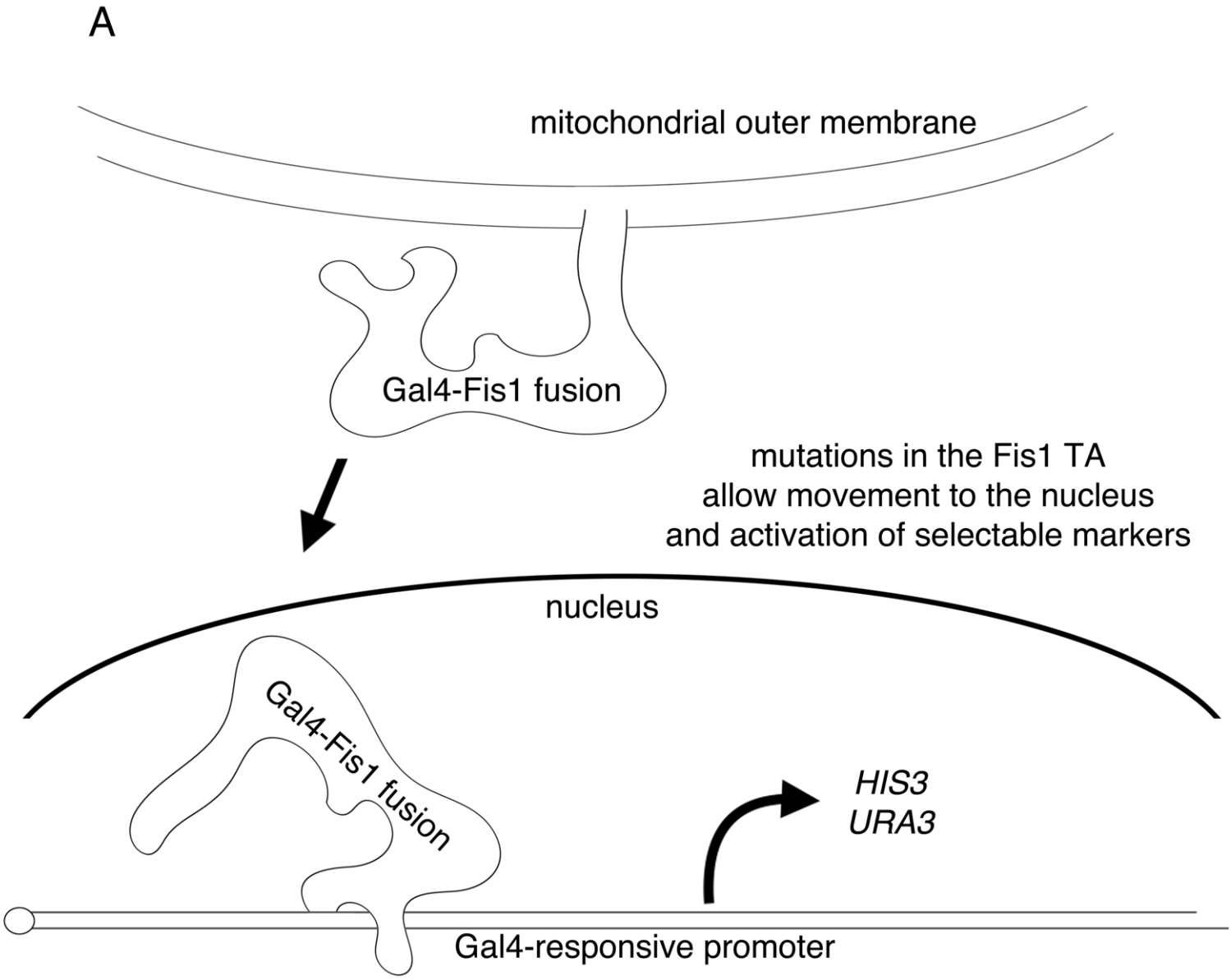

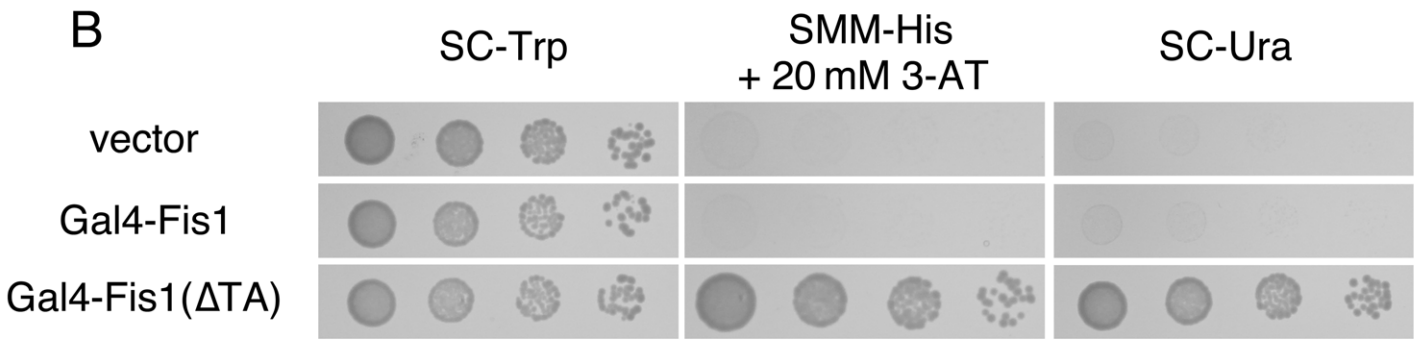

Figure 1

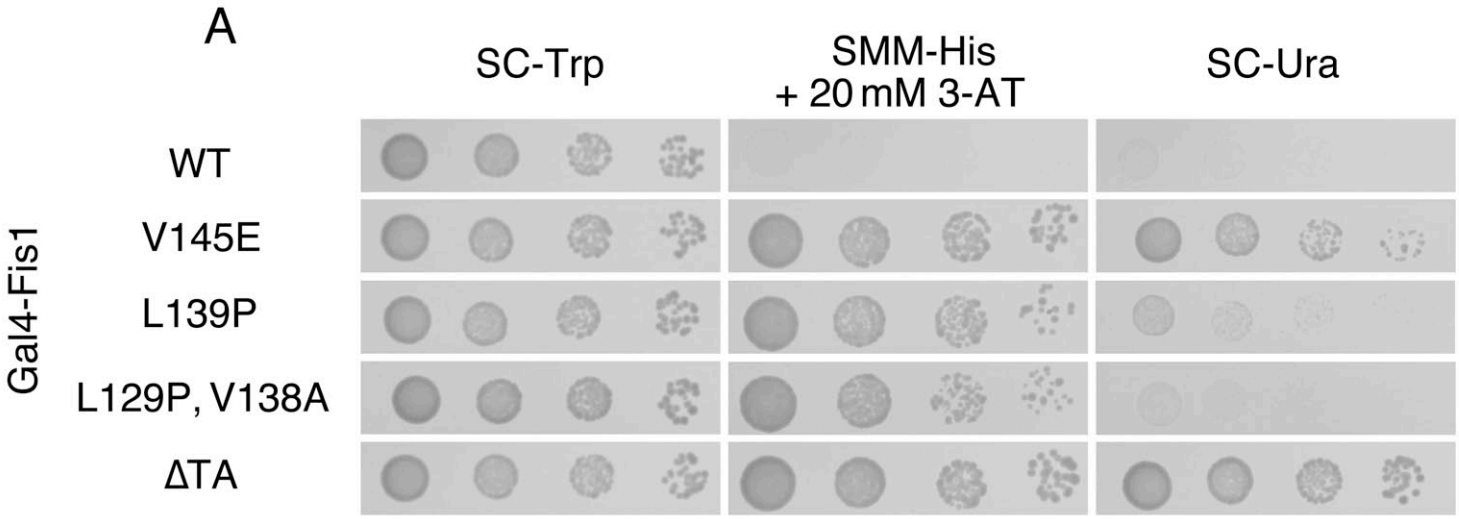

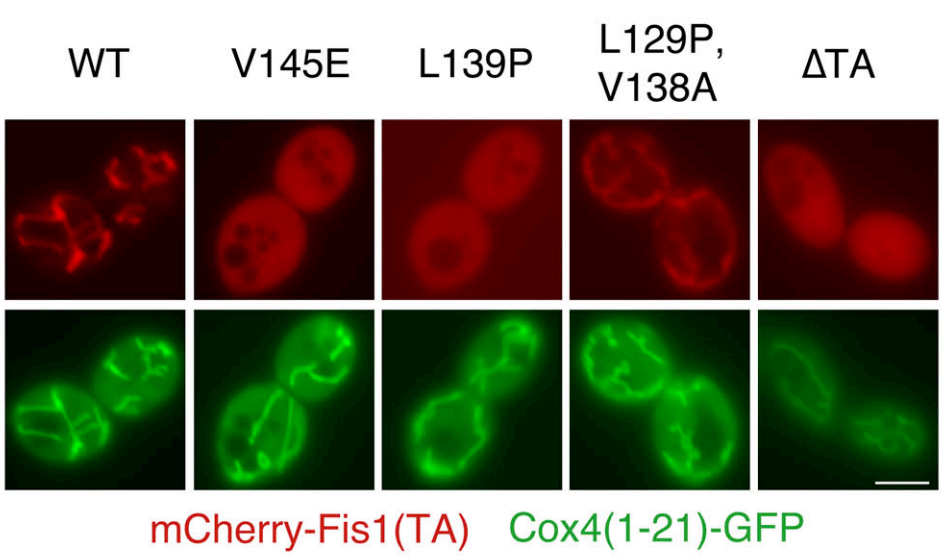

Figure 2

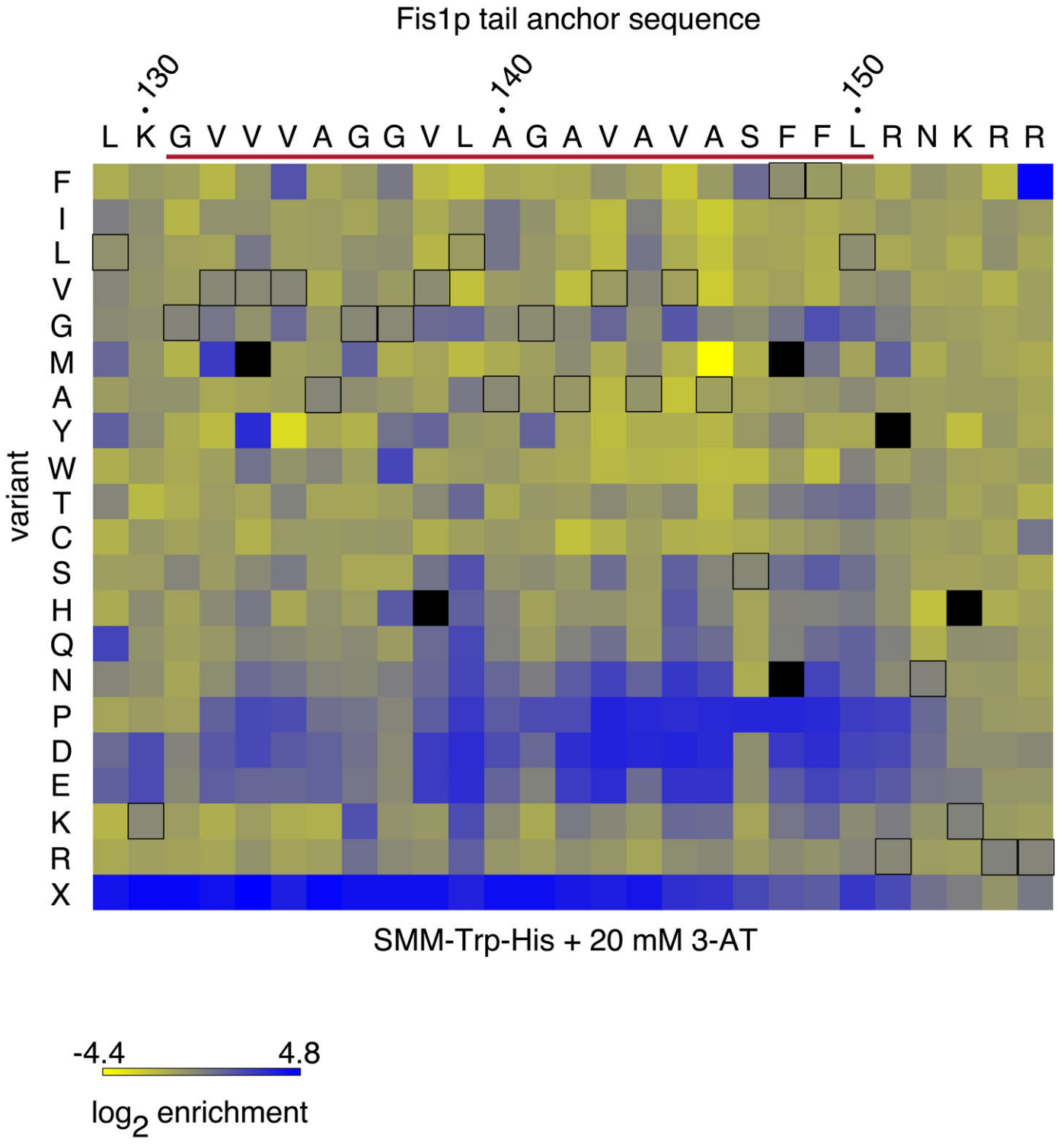

Figure 3

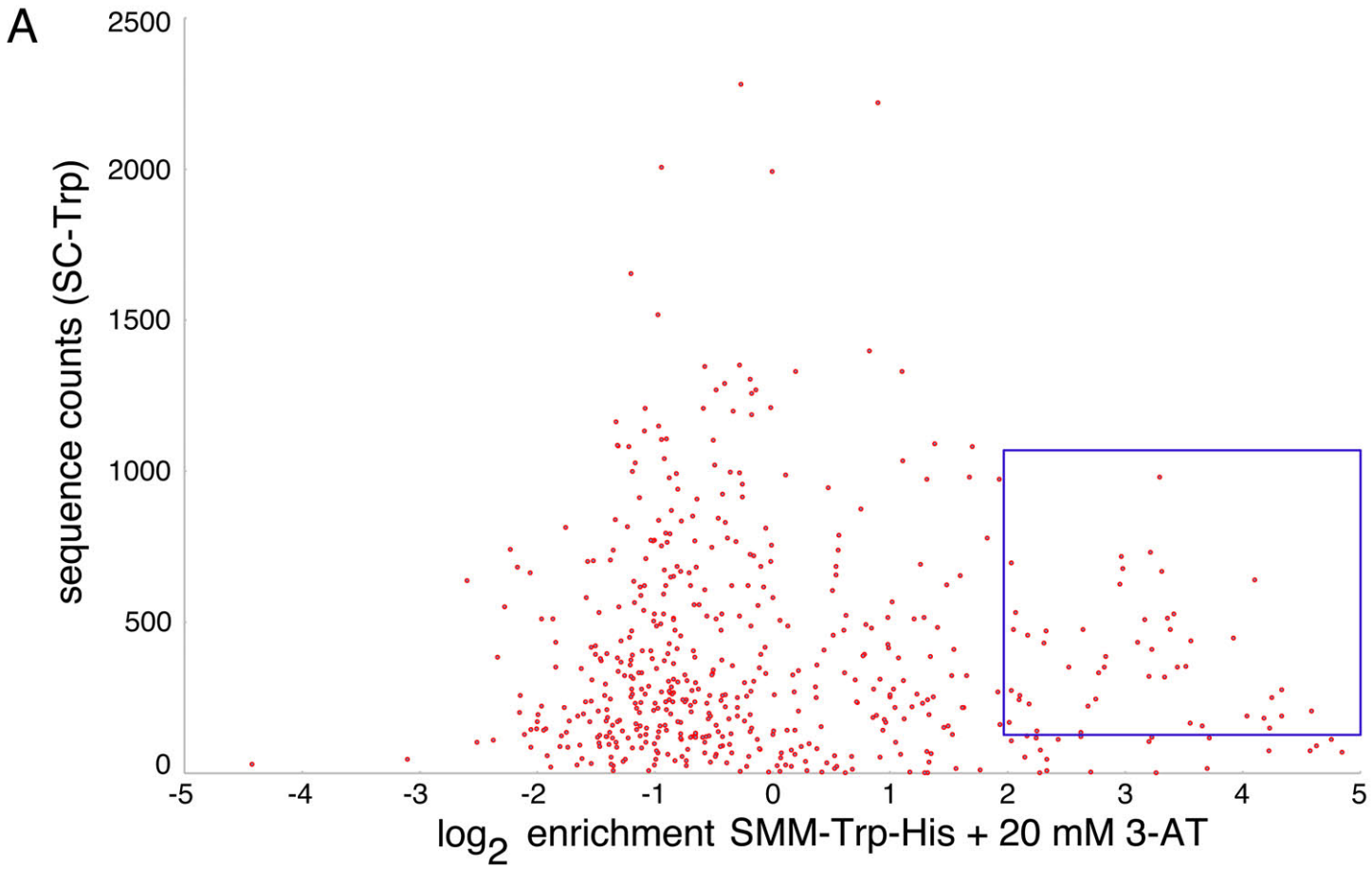

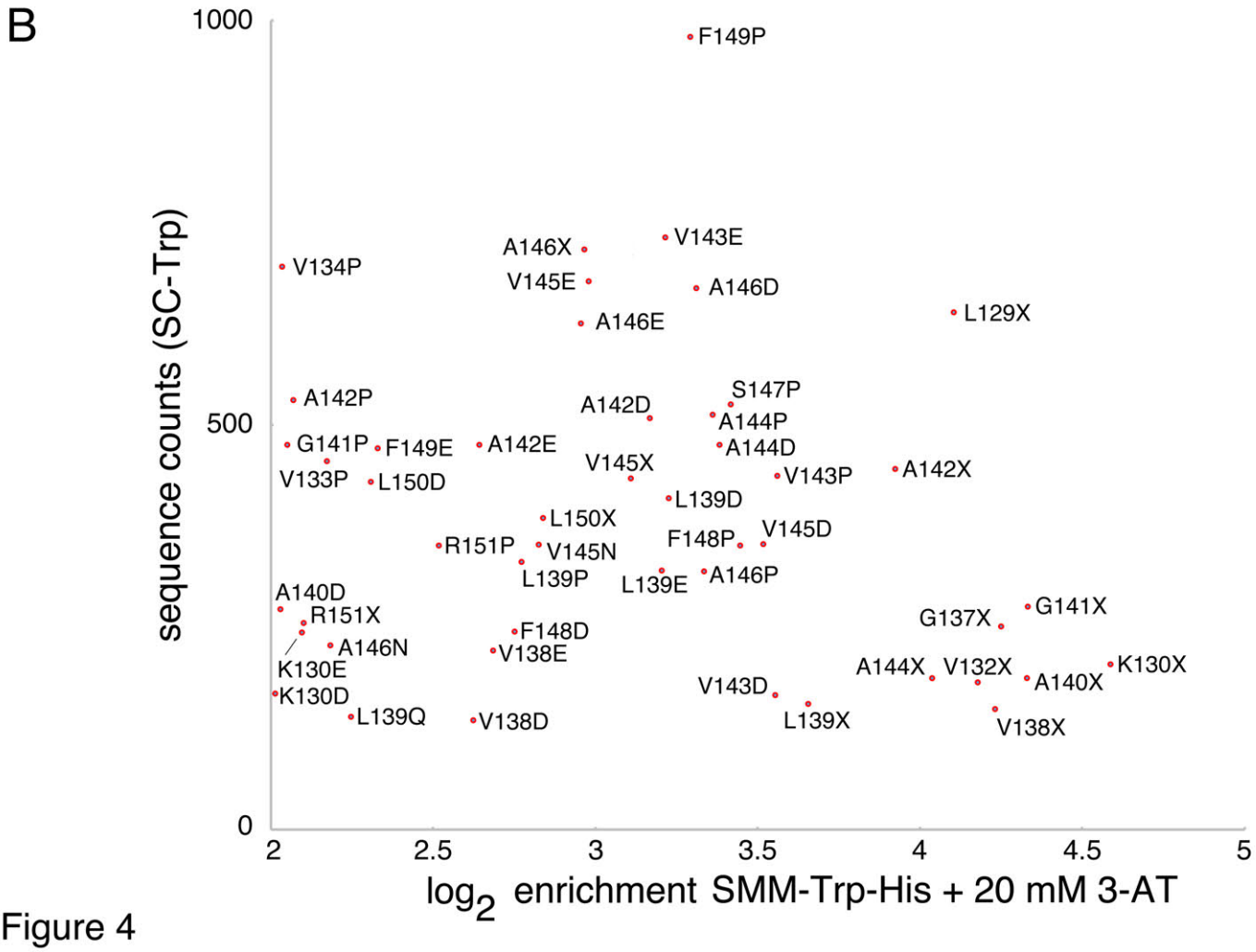

Figure 4

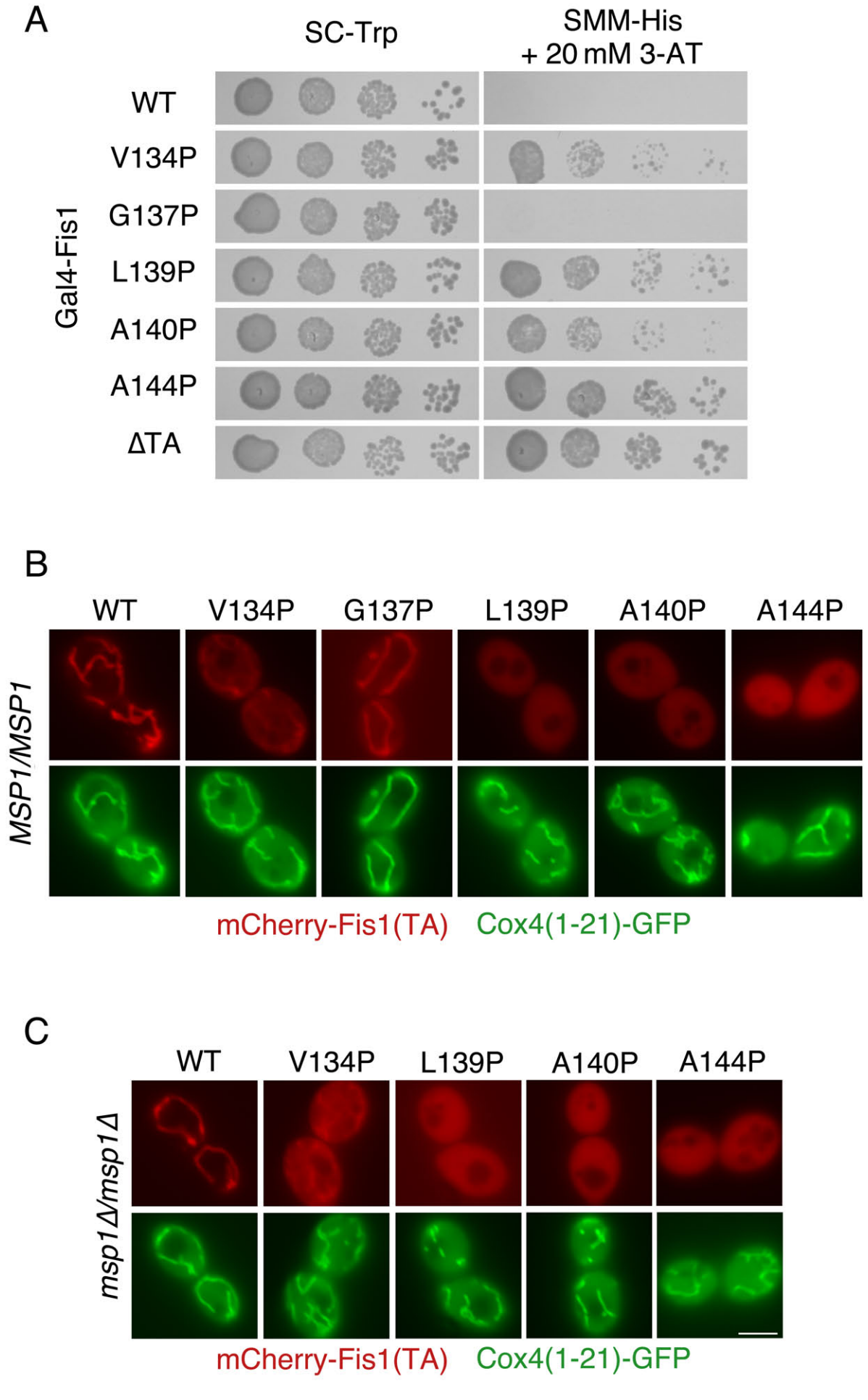

Figure 5

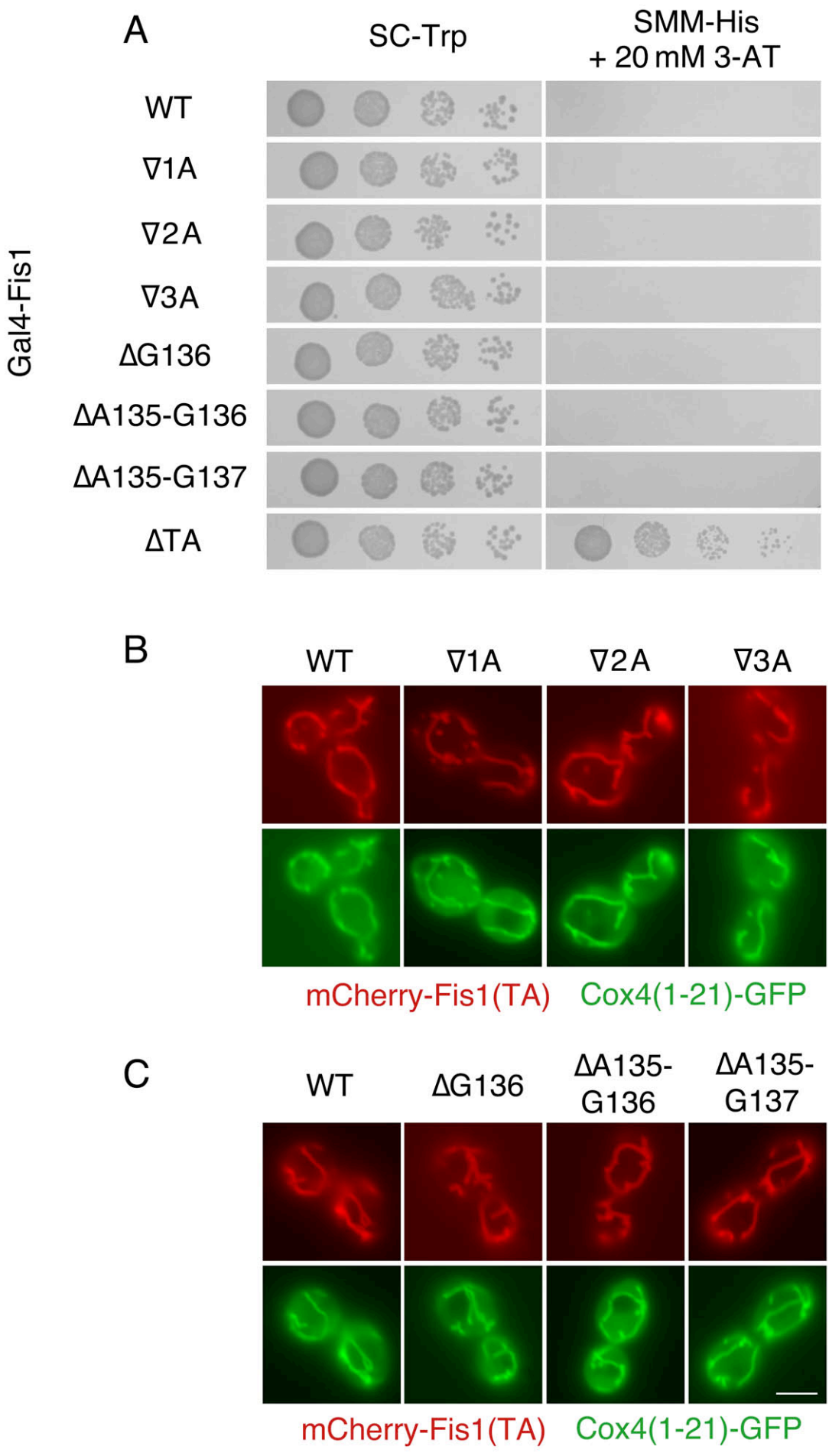

Figure 6

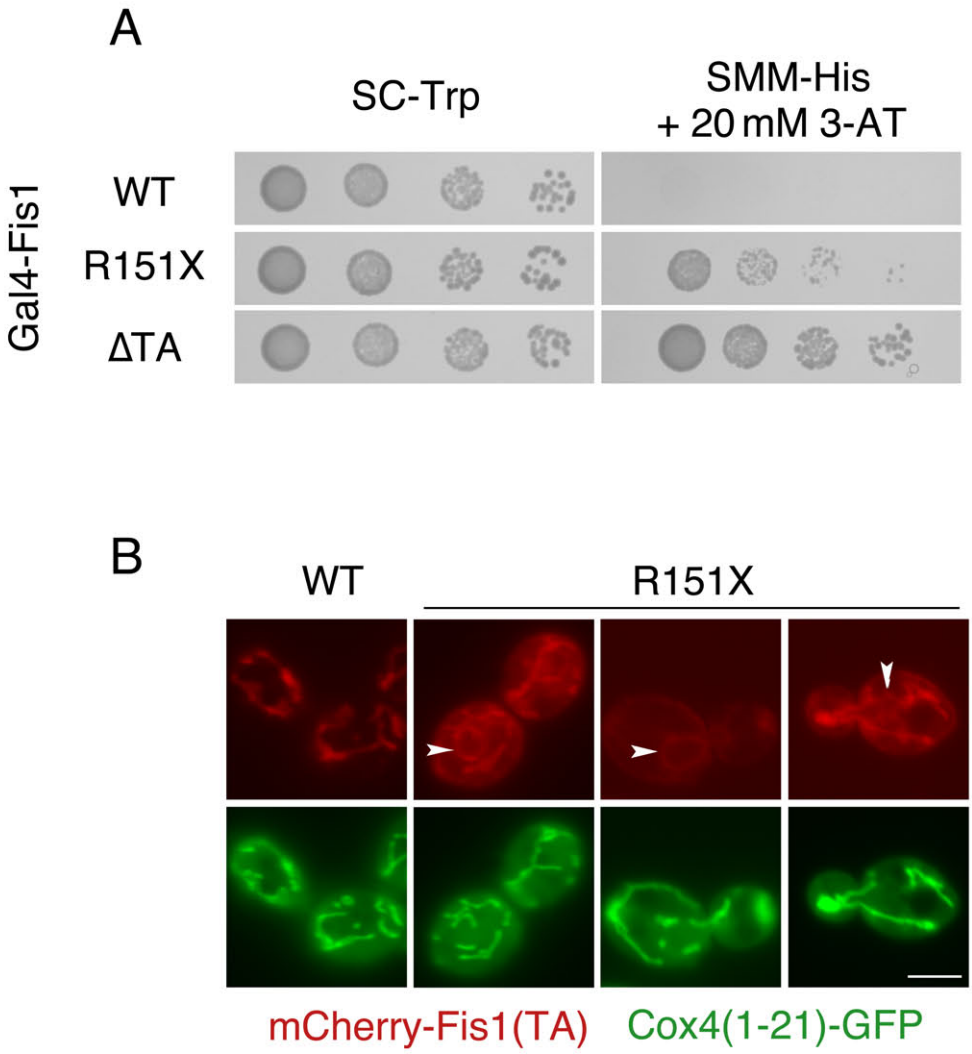

Figure 7

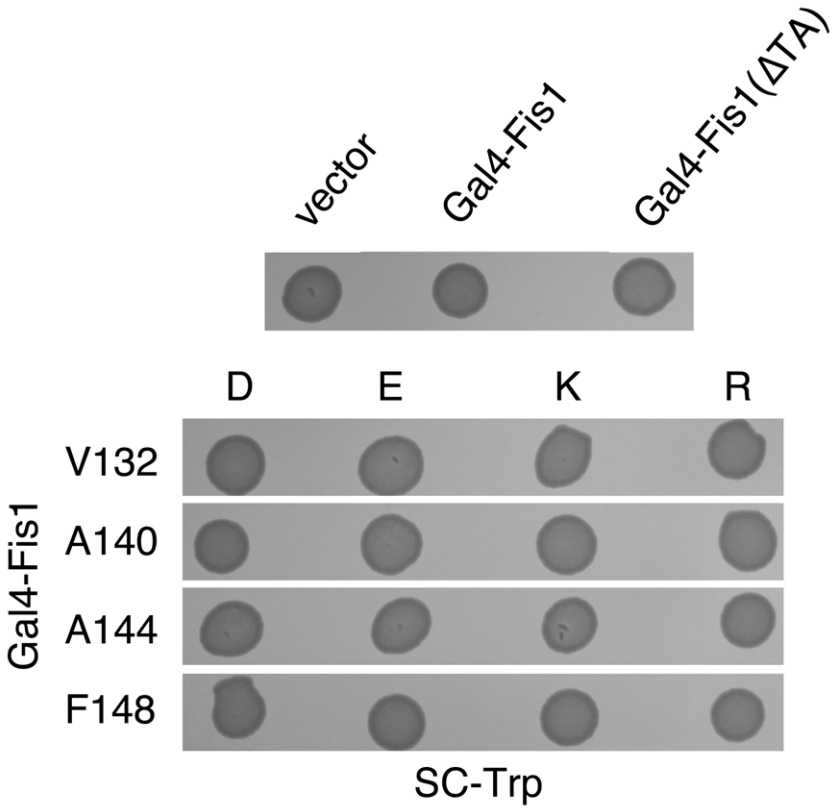

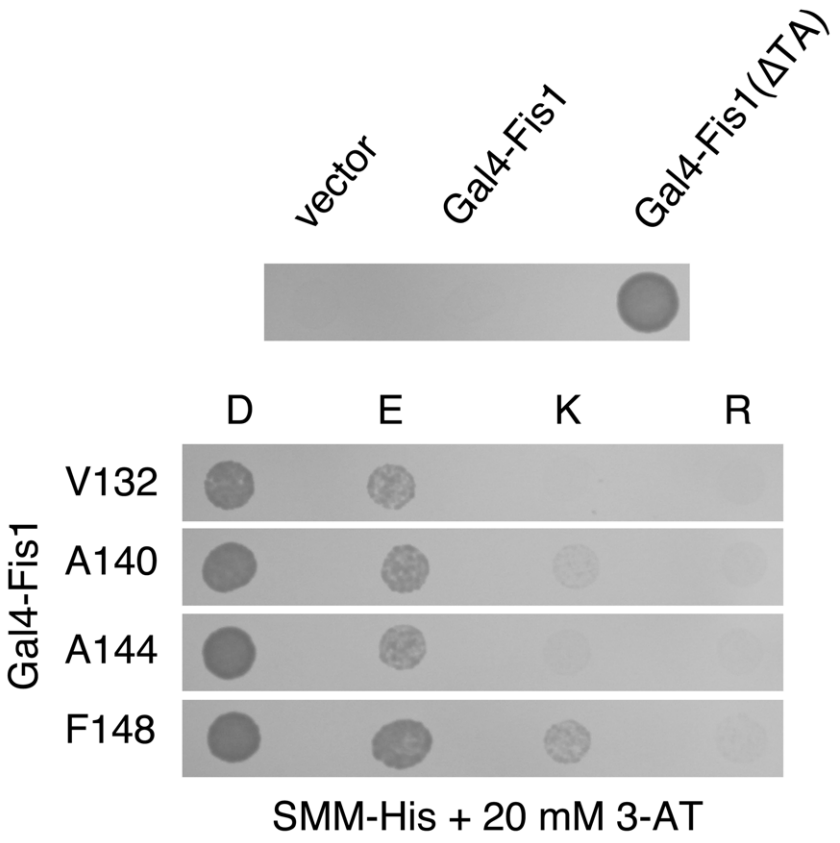

Figure 8

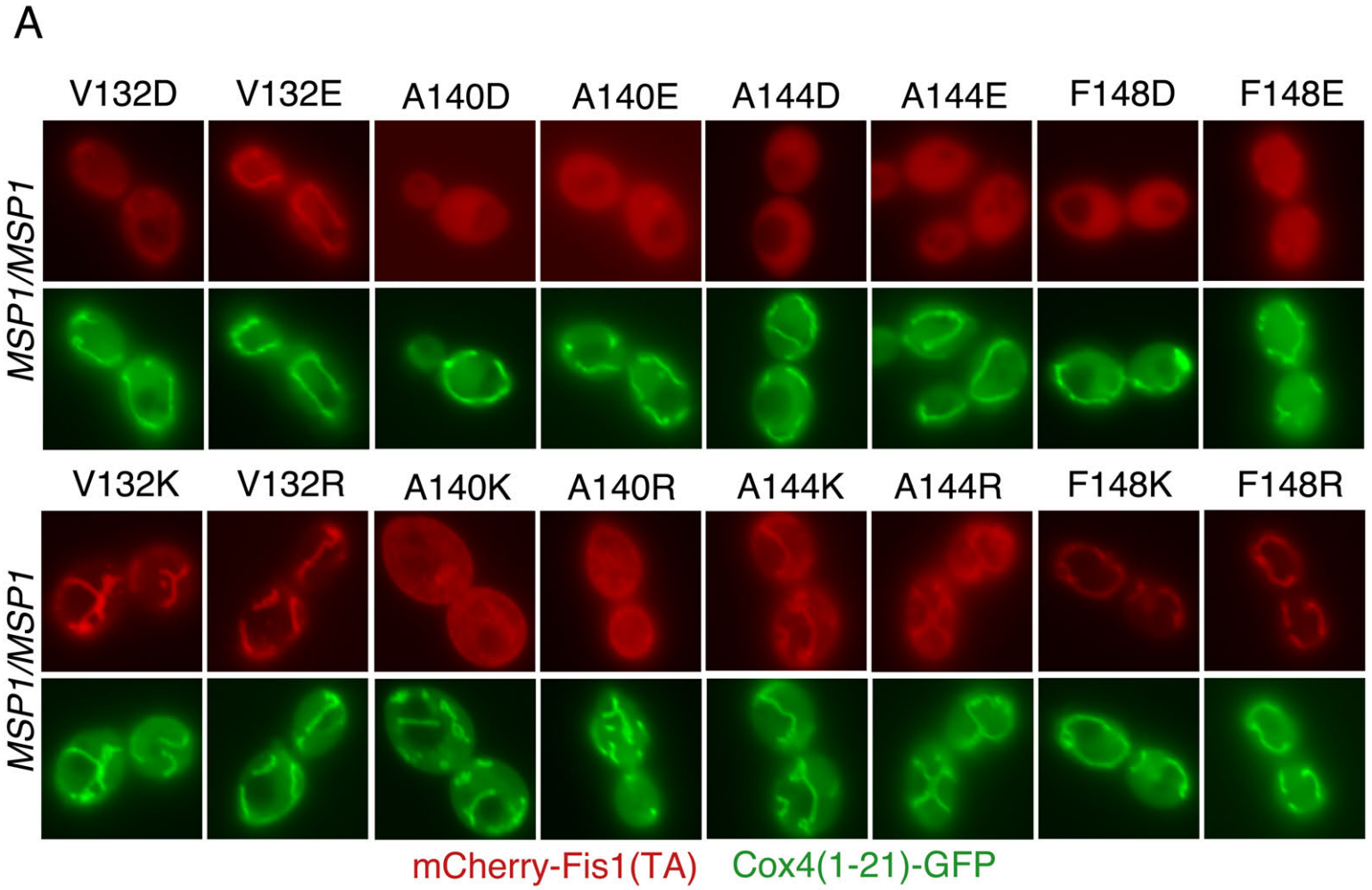

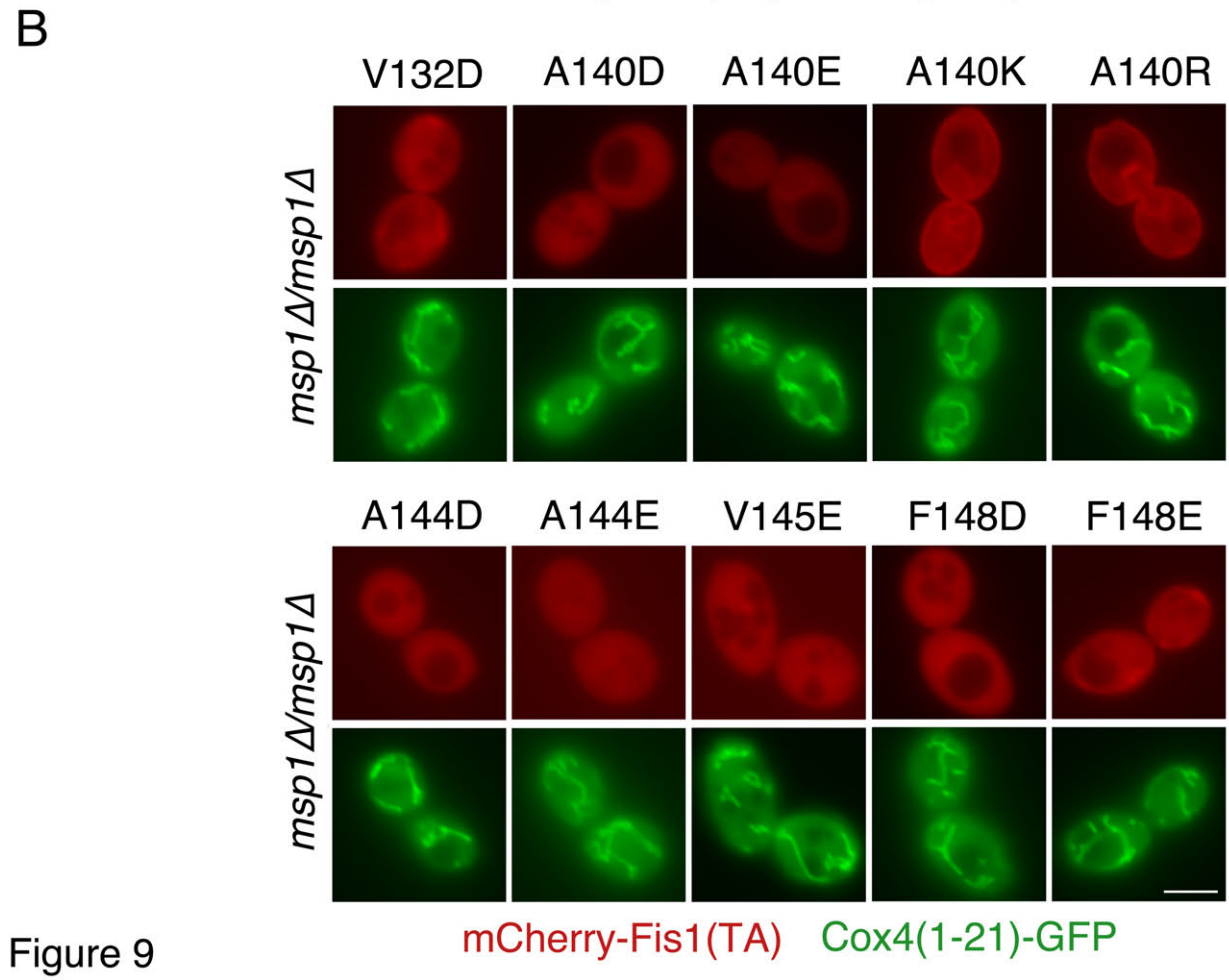

Figure 9

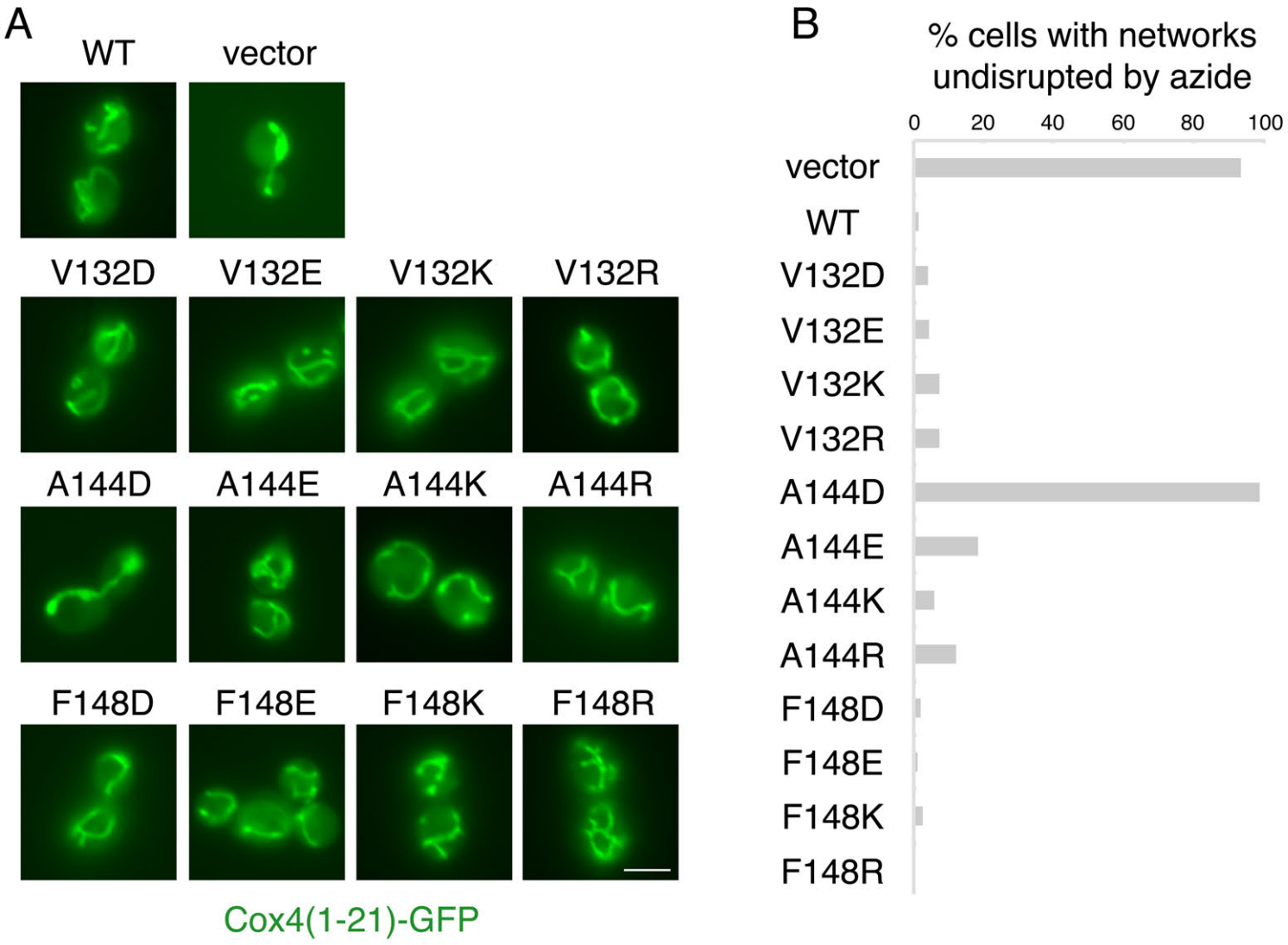

Figure 10

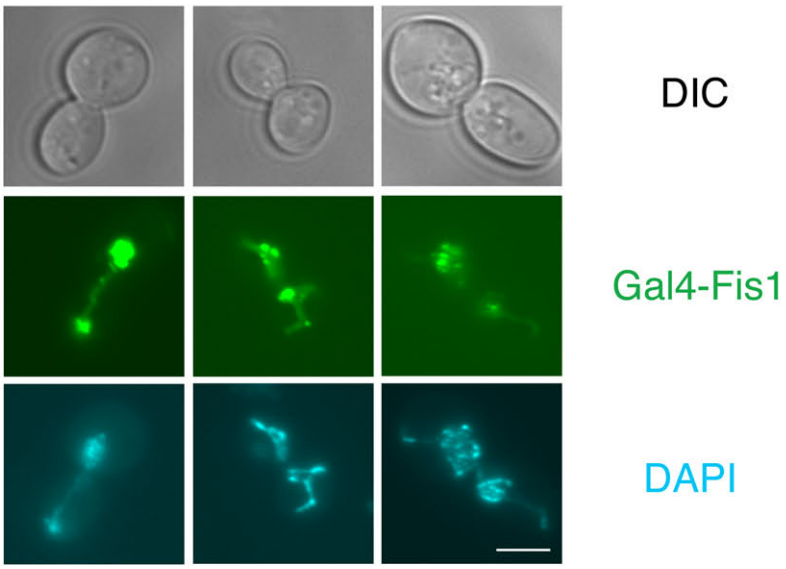

Figure S1

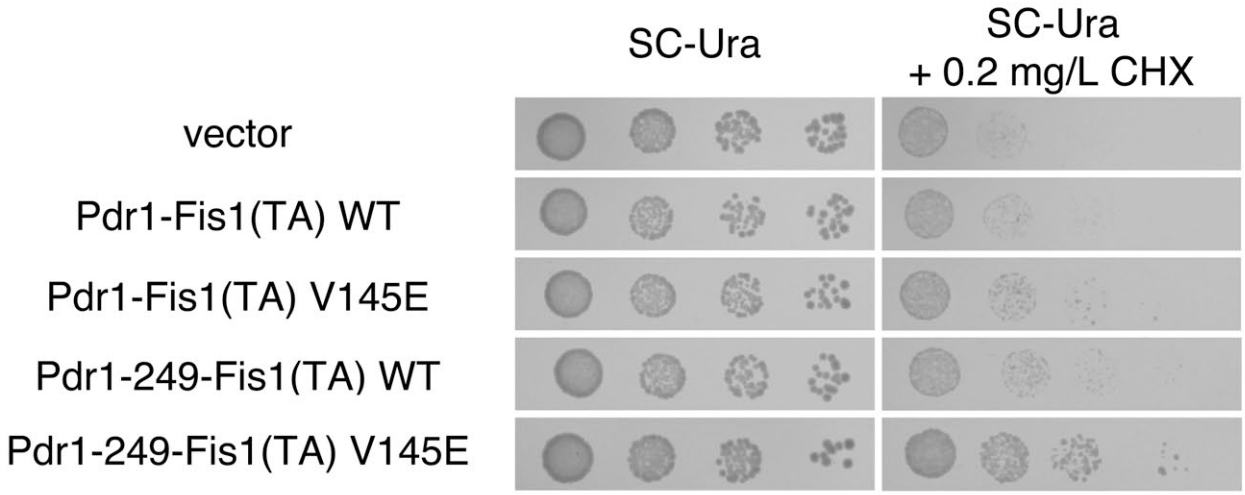

Figure S2

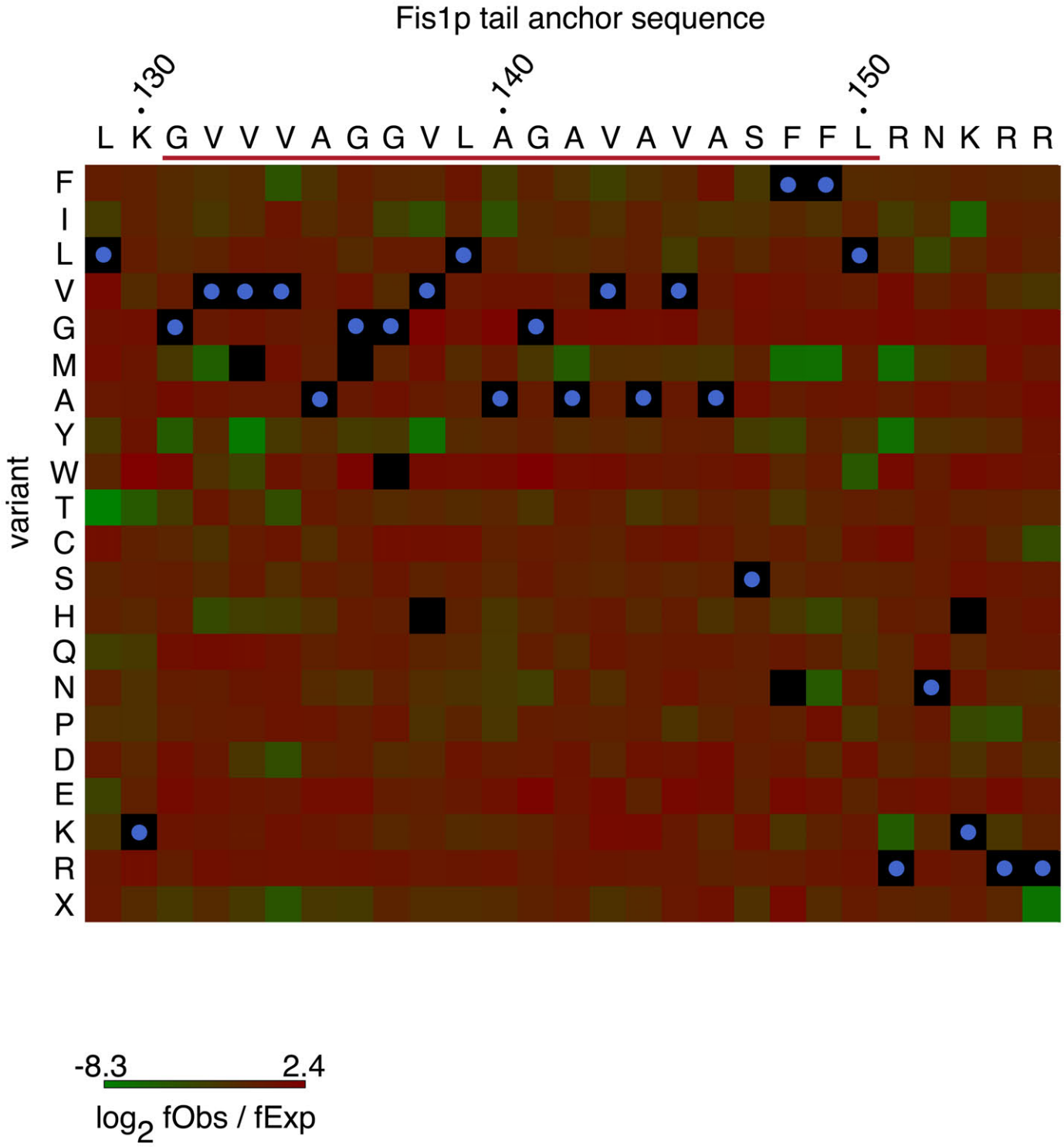

Figure S3

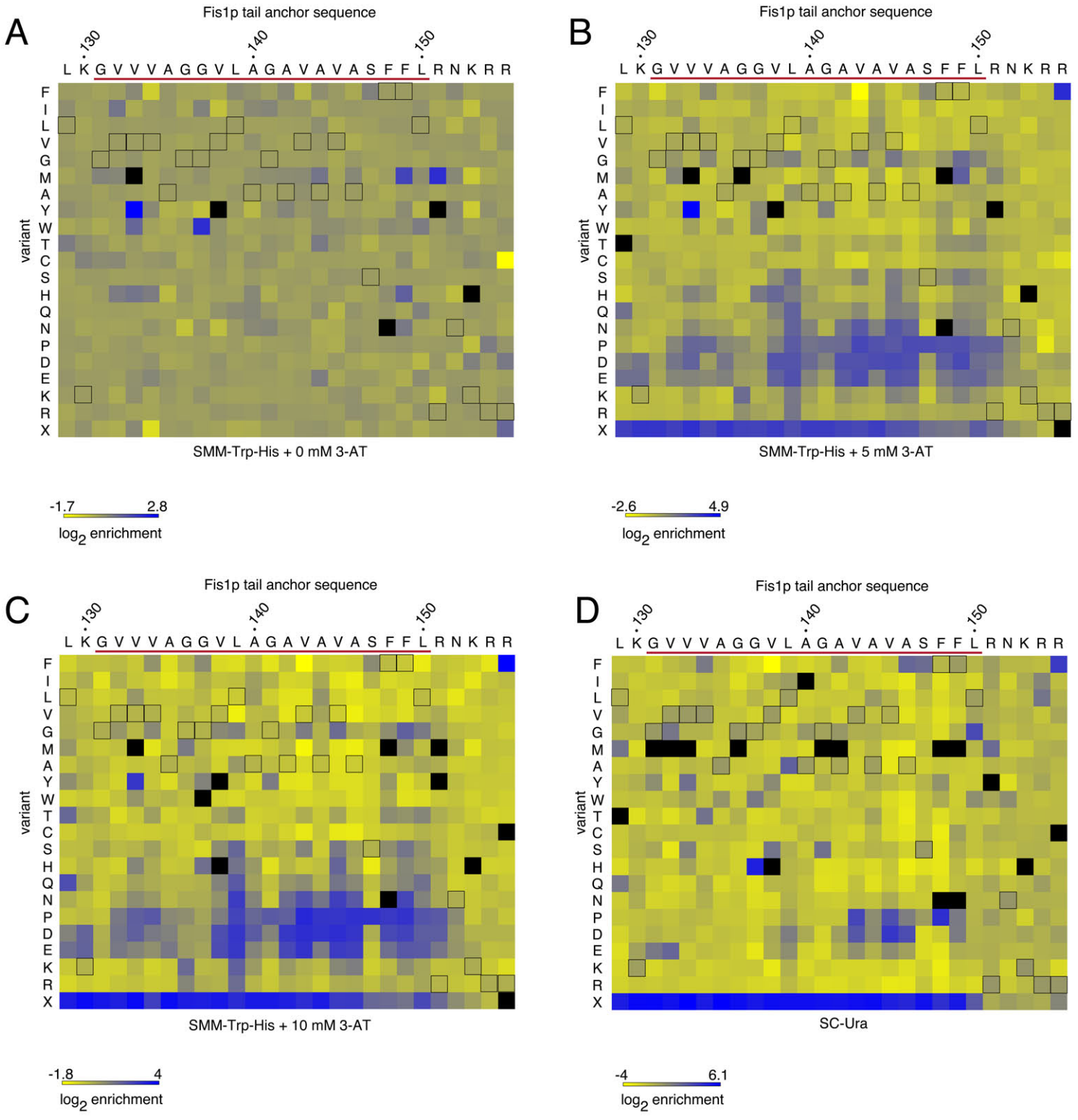

Figure S4

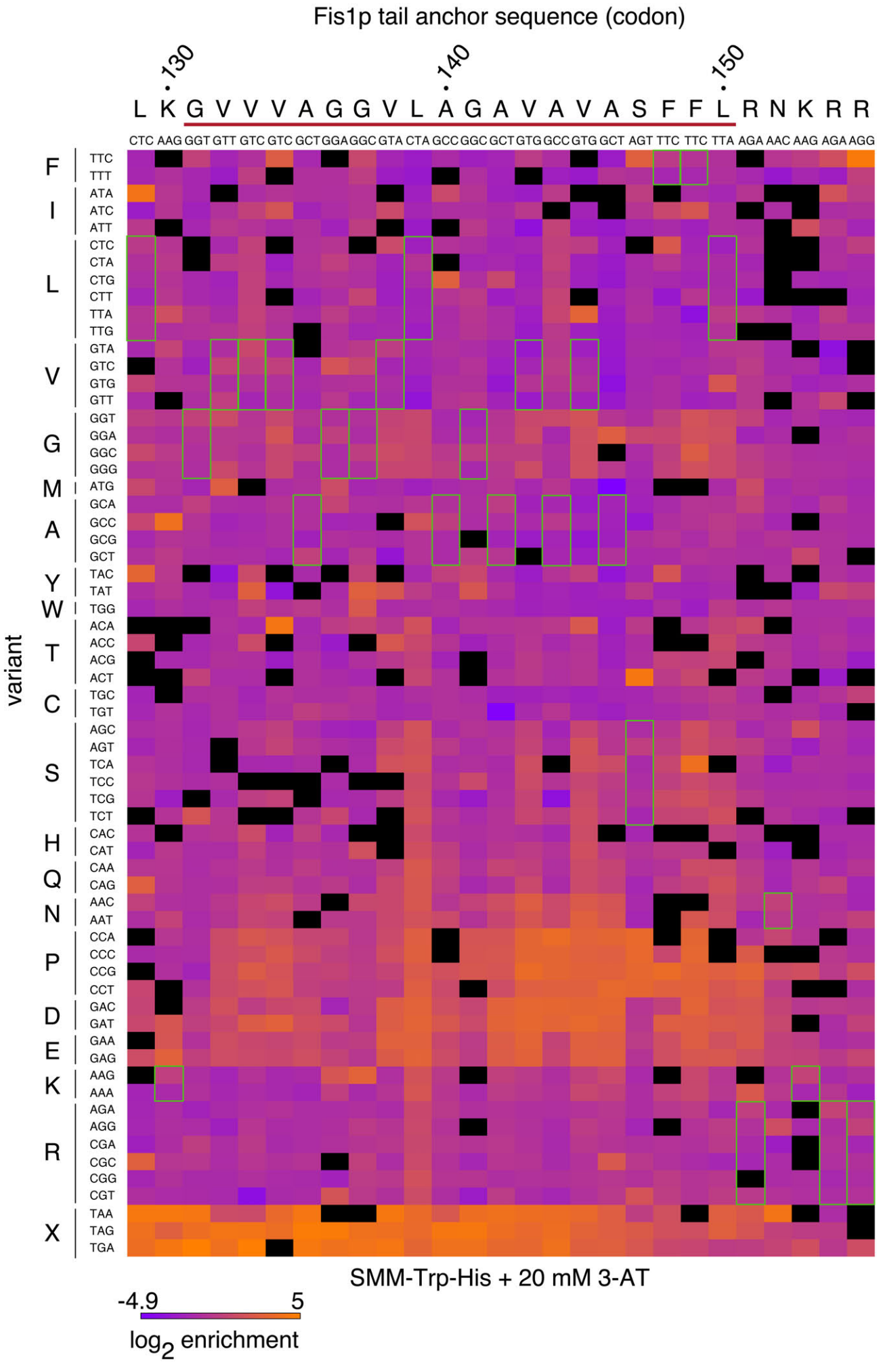

Figure S5

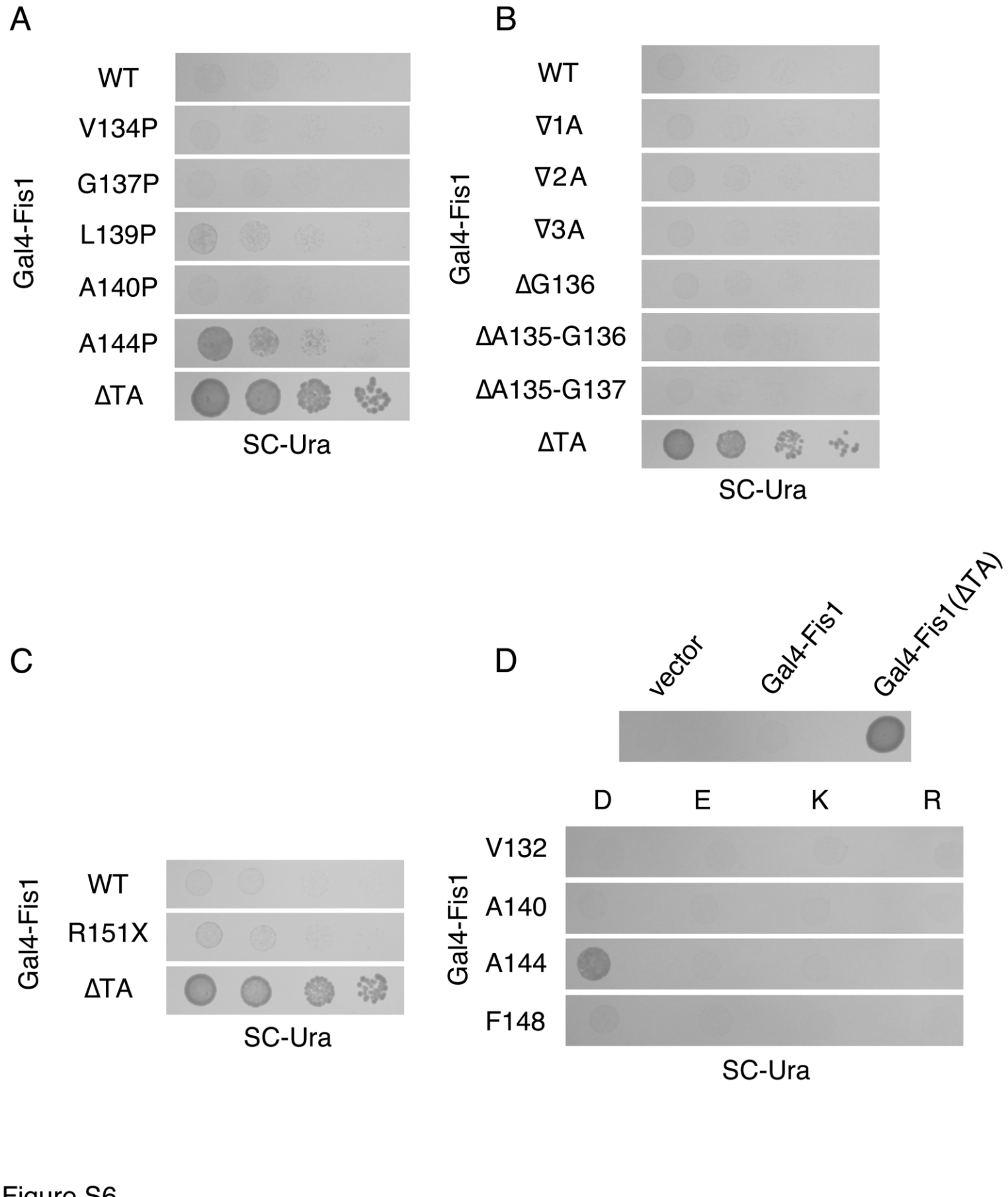

Figure S6

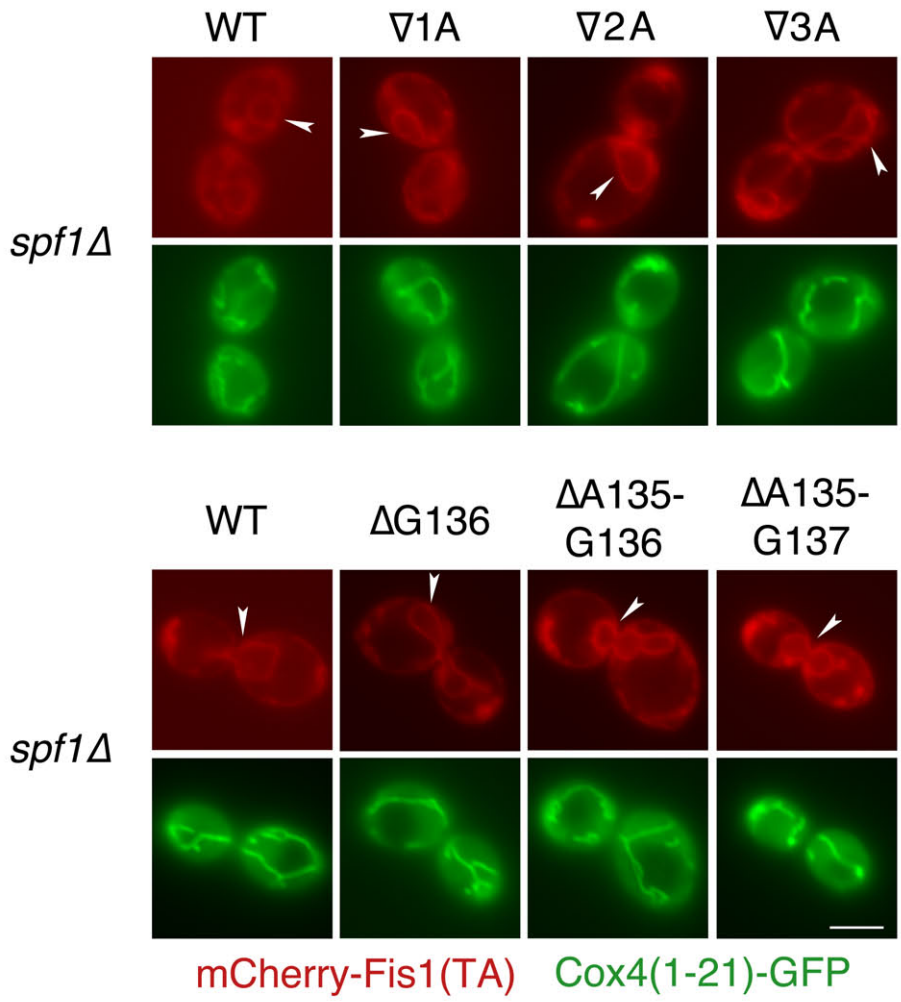

Figure S7

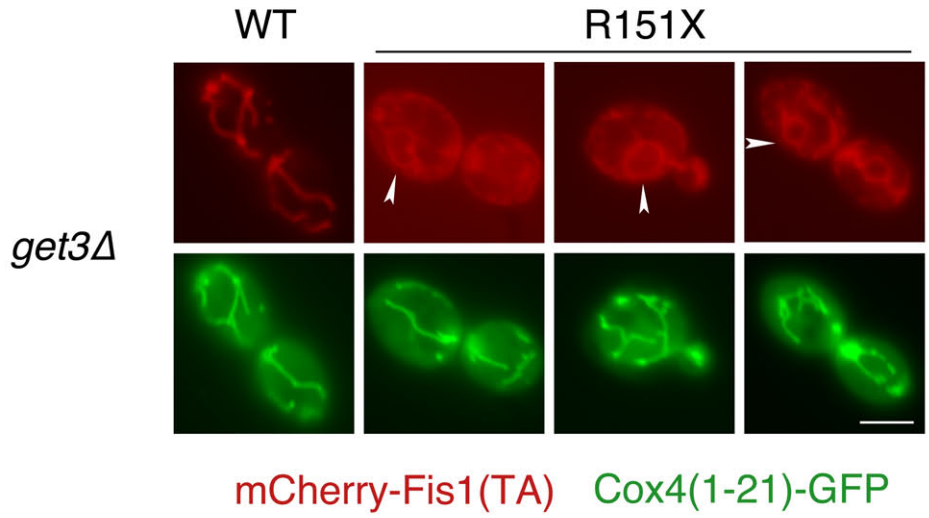

Figure S8

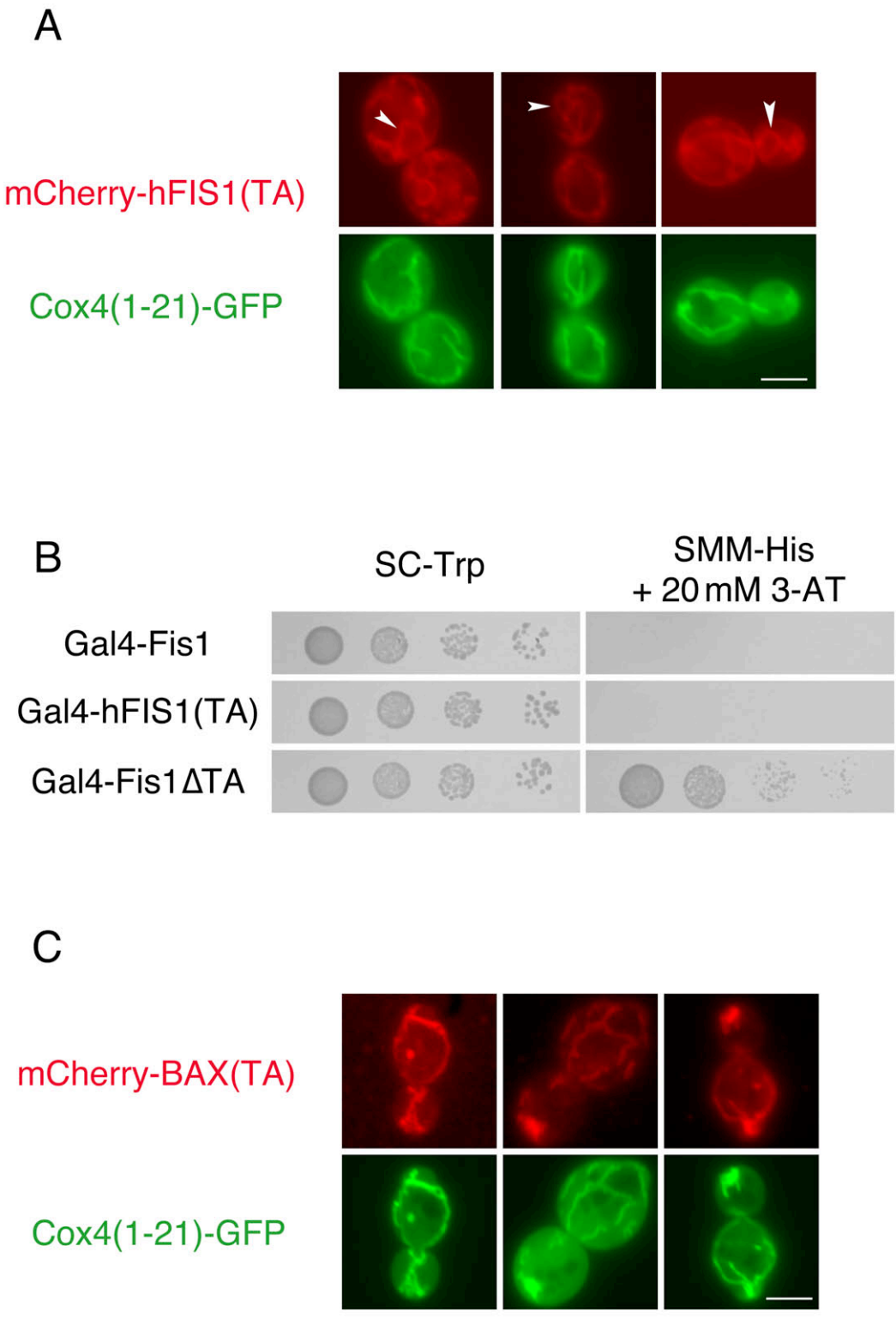

Figure S9

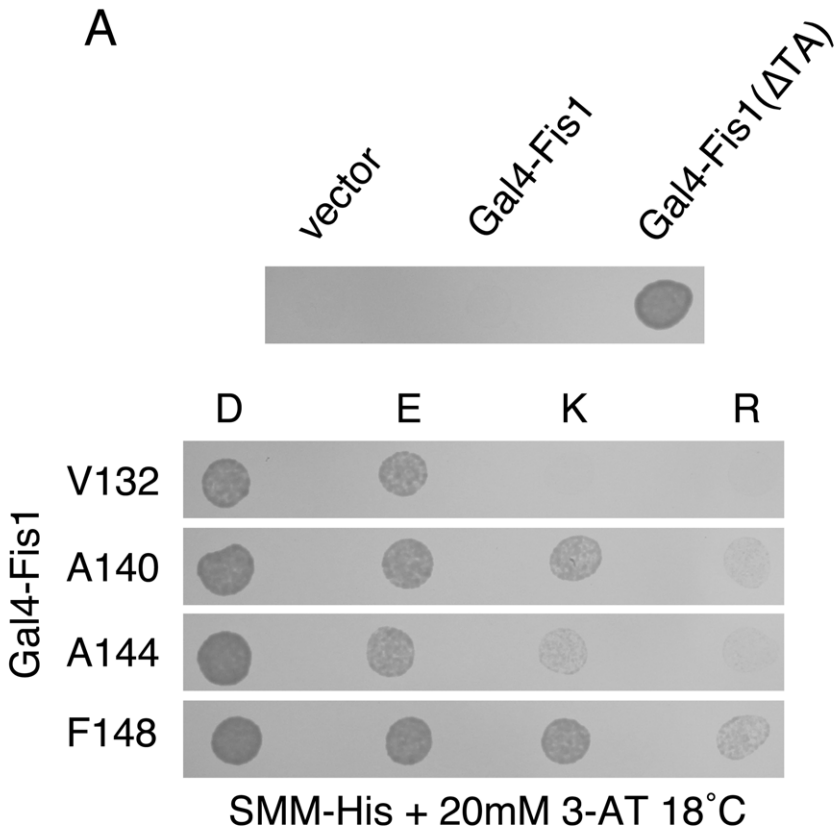

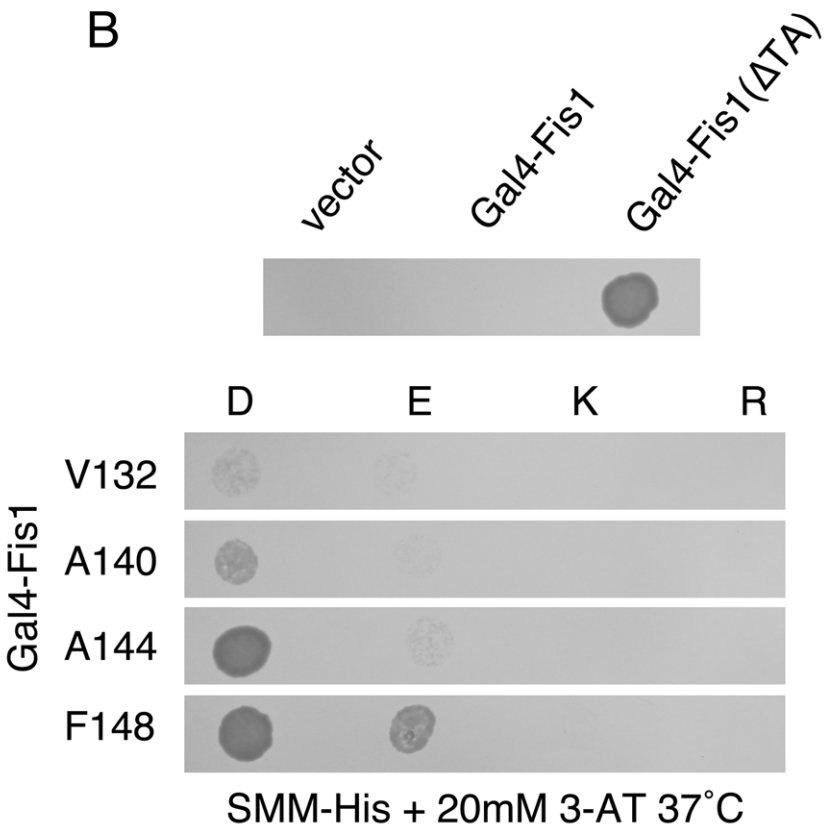

Figure S10

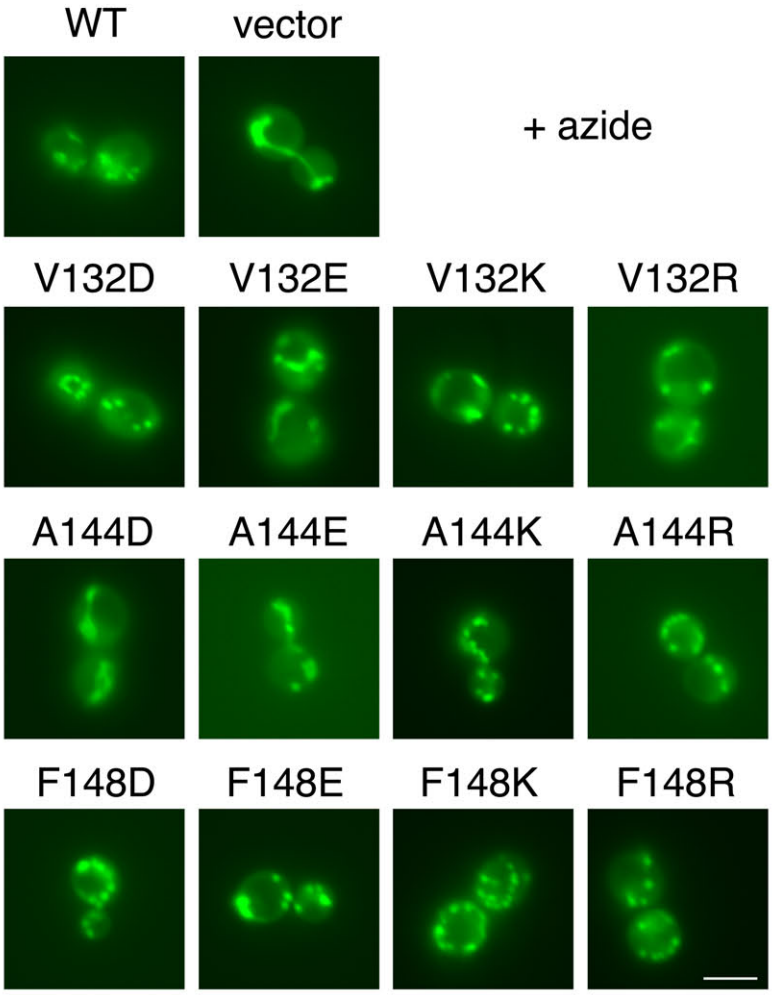

Figure S11